Offshore Methane Hydrates: Optimal Recovery and Utilization

FINAL REPORT

TEAM II

YANMING GONG

VENKATA PRADEEP INDRAKANTI

PETER L PEREZ

SCOTT POWERS

RAMYA VENKATARAMAN

TABLE OF CONTENTS

TABLE OF FIGURES

1 Abstract

This report assesses the production and utilization of natural gas from an offshore methane hydrate reservoir located at Hydrate Ridge, 100 Km away from the Oregon coast, where substantial amounts of natural gas in the form of hydrate have been identified.

The following pages describe our approach to recover and utilize methane from gas hydrates. Details of the production system envisaged, slope stability under production and subsequent utilization of the methane thus produced are discussed. A Net Present Value Economic Analysis based on the methane production rate is presented for various utilization scenarios.

2 Site\Resource Characterization

The amount of gas (from gas hydrates) in place at southern Hydrate Ridge (including the flanks and the adjacent slope basin) has been estimated to be 270-500 billion cubic feet (BCFT)[1]. The gas hydrate resource at the summit (having the maximum gas hydrate saturation in the pore space at Sites 1249 and 1250) was calculated to be 14 billion cubic foot (BCFT) , which is equivalent to a USGS Field size class 9[2]. It has to be noted here that the recoverability of the resource is not implicit in the above classification. Offshore gas hydrate bearing clayey sediments such as those found at Hydrate Ridge have permeability of ~10 mD (milli darcy) Appendix(Upstream) , which compares to that of a tight gas reservoir (~0.1 mD[3]). Whereas tight natural gas reservoirs can be fractured to increase the permeability, some of the challenges in offshore gas hydrate recovery are high exploration and development costs and maintaining the fracture open\providing a more permeable flow path to the gas as dissociation proceeds.
Gas hydrate occurs as ~20% of the pore space from the seafloor to the BSR at the summit[4] and as 1-3% of the pore space at other sites. The lithologies do not vary very widely across sites.[5] From this preliminary site characterization, it is evident that the summit would be the most economically attractive area to drill.

[1] Literature Review, Team II
[2] http://tonto.eia.doe.gov/FTPROOT/modeldoc/m063(2004).pdf , page 3-D-5.
[3] Cox S.A., Gilbert J.V. et al., Reserve Analysis For Tight Gas, SPE 78695, presented at the 2002 SPE Eastern Regional Meeting held in Lexington, Kentucky, 23-25 October 2002.
[4] Trehu AM et al., Three-dimensional distribution of gas hydrate beneath southern Hydrate Ridge: constraints from ODP Leg 204, Earth and Planetary Science Letters, 222, 845-862, 2004.

[5] A comparison of smear slide data from Sites 1244 and 1249 did not reveal any particular variation in the clay:silt ratios.

3 Production system

3.1 Rate limiting steps in recovery

The dimensionless numbers from which rate controlling parameters can be obtained are described in detail in the Appendix and the Notations section. There can be three main rate limiting factors to gas hydrate dissociation: Fluid flow, Heat transfer and Intrinsic Kinetics. It is known that the intrinsic kinetics of gas hydrate decomposition is much faster than the time scale of heat and momentum transfer. The relative importance of thermal conductivity and permeability on dissociation is given by $\frac{\alpha_1}{P_e a_1}$. Typical sediment thermal conductivities at Site 1249, 1250 Hydrate Ridge are 1 W/mK[6]. The bulk density of the sediment is ~1.6 g/cc[7] and the specific heat is taken to be ~2.5 KJ/kg K[8], which give a thermal diffusivity of 2.5E-7 m^2/s. The permeability of clays is calculated to be ~10^{-14} m^2 as shown in the Appendix A. Using viscosity of methane as ~10^{-5} Pa-s, porosity as 0.65, and the equilibrium pressure to be 8 MPa at 286 K[9], the ratio of the thermal and darcian diffusivities is ~2E-5. This shows that the thermal inertia of the sediment at Sites 1249, 1250 ultimately limits the rate of hydrate dissociation. This has a compounded effect as not only the kinetics of dissociation (i.e. Arrhenius prefactor term) but also the thermodynamics are controlled by heat transfer and not fluid flow. This is an important consideration for any optimal hydrate recovery scheme. We present a brief calculation of how electrical heating might be used to heat the sediment.

3.2 Estimates of Drilling & Exploration Costs

Based on the water depth, resource concentration and field size site 1249 can be classified as a USGS class 10 which is used as the basis for technology assumptions in OSS[10]. The production platform chosen to drill at the summit is an FPSO system (semi-submersible) with onboard production and processing capability. It was mainly chosen for two reasons 1. Ability to position dynamically- this prevents platform instability issues caused by sediment displacement in the GHSZ. 2. A semisubmersible has large operating depths and can be used in waters > 3000 ft deep and has a shape that tends to dampen wave motion, thus can be used in areas that show high wave motion.

The main steps are involved in production from a prospective field are exploration drilling program, fabrication and installation of the development/production platform development, pre-drilling during construction of platform, construction of gathering system, production operations and finally, field abandonment.

The average drilling rate in the GHSZ & BSR is given by
Rate (ft/day) = 800-0.58* drilling depth, for total drilling depths less than10,000 ft.

---

[6] From http://iodp.tamu.edu/janusweb/general/dbtable.cgi?leg=204&site=1249
[7] From http://iodp.tamu.edu/janusweb/physprops/gradat.cgi?leg=204&site=1249&hole=F
[8] Abu-Hamdeh N.H., Thermal properties of soils as affected by density and water content, Biosystems engineering ,[1537-5110], 2003,86(1) p: 97
[9] From http://www-odp.tamu.edu/publications/204_IR/chap_01/c1_f3.htm
[10] http://tonto.eia.doe.gov/FTPROOT/modeldoc/m063(2001).pdf

Based on this equation the drilling rate at the summit was calculated to be 467 ft/day. Based on the depressurization model used for production, about 32 subsea wells each producing 0.1 MMSCFT/d are required for a daily production rate of 3 MMCFT/d. A well bore diameter of ~0.1 m was selected. We think that details of the casing calculations are beyond the scope of this project. Since a detailed economic analysis of gas production involves too many parameters, it is not possible to consider every one of them. For the purpose of brevity, some general assumptions have been made and only the most important factors have been considered.

The OSS assumes almost no cost for a subsea well, since these are generally tied back to an existing production system. The main cost here is only that of the pipeline used to transport the gas to the production platform. For subsea systems that do not produce to a fixed platform a drilling template must be used that connects to a group of wells. The cost of the subsea template is given by:

Cost of Subsea Template = 2,500,000 * NTMP, where NTMP is the number of wells per template. 4 drilling templates, each connected to 8 wells are used in our case. This brings the total cost of templates to $ 10 Million.

The exploration cost from a semisubmersible platform given by the equation:

Exploration cost: 2,000,000 + 1,825*WD + (0.01*WD + 0.045*ED - 415)*ED (1.1)

Where WD = water depth & ED = exploration drilling depth, was calculated to be around $ 6.65 Million/well.

The time required to drill development wells is much lesser than for exploration wells. A dry development well drilling cost does not include costs to complete and equip the well. The cost of successful development drilling is calculated by summing the dry development well drilling costs and the well completion and equipment costs. Typically, Dry Development Drilling Cost For water depths less than or equal to 900 meters is given by,

Cost= 1,500,000 + (1,500 +0.04*DD)*WD + (0.035*DD - 300)*DD (1.2)

Where, WD = Water Depth, feet, DD = Development Drilling Depth,

For our production model we assume no dry wells.

Well Completion and Equipment Cost ($/well) at a Water Depth of ~ 2700 ft and drilling depth of <10,000 ft is ~ $ 1.9 Million.

For a typical offshore well at a water depth of 800 m, the above equation yields a total cost of $ 6.65 Million/well. However based on the team's personal communication with Dr. Robert Watson (Prof. of Petroleum and Natural Gas Engineering, PennState University) the cost of drilling and well completion for a well at the summit in the hydrate ridge can be lowered to ~ $ 1 Million/well[11]. This is mainly attributed to the high drilling rates possible through the soft sediments in the GHZ. Total development drilling costs therefore come to ~ $ 32 Million. Rotary drilling with top drive can be used and the drilling fluid for hydrate sediments can be salt water, since density of the fluid ~ density of formation sediments[12].

[11] Personal communication – Dr. Robert Watson, Professor of Petroleum and Natural Gas Engineering, Dept. of Energy and Geo-Environmental Engineering, PennState University – 11/20/2004.

[12] http://tonto.eia.doe.gov/FTPROOT/modeldoc/m063(2001).pdf

For a conventional offshore gas field with production capacity of 0 - 20 MMCFT/day, the cost to install production equipment on the development structure is given the equation:

PRCEQP = (0.675 * QMXGAS) * 1,000,000 / NSTRUC

TOPEQP = (0.950 * QMXGAS) * 1,000,000 / NSTRUC (1.3)

Where, PRCEQP is the processing equipment cost

TOPEQP is the topside equipment cost

QMXGAS is the max. gas production value in MMSCFT/d

NSTRUC is the No. of structures

For platforms producing primarily gas, the top total costs of the topside facility is represented by the sum of the processing equipment costs (PRC EQP) and the topside equipment cost (TOPEQP). PRC EQP for a QMXGAS OF 3 MMSCFT/d was calculated to be $ 2.02 Million. TOPEQP cost was calculated to be is $ 2.85 Million. Therefore the total cost to install production equipment is $ 4.87 Million.

The annual operating cost includes the following items:

- Primary oil and gas production costs,
- Labor,
- Communications and safety equipment,
- Supplies and catering services,
- Routine process and structural maintenance,
- Well service and workovers,
- Insurance on facilities, and
- Transportation of personnel and supplies.

It can be calculated using the equation,

Cost ($/structure/year) = 1,265,000 + 135,000*NLST + 0.0588*NLST*WD*WD. (1.4)

Where NLST is the number of slots.

Since we have only one structure, the operating cost per annum as calculated by the above equation is $ 4.5 Million.

In subsequent sections, two different scenarios have been considered for the end use of methane from methane hydrates- conversion of methane back to methane hydrates transportation in the form of solids and methanol synthesis by methane reforming and gas to liquid processing. The economics of both scenarios were evaluated and respective average costs per unit methane produced have also been reported.

3.3 Depressurization Model

3.3.1 Assumptions

Under this model, the model behaves as a closed system with no boundaries. The following assumptions are considered[13]:

1. Hydrate dissociation occurs as soon as the reservoir pressure drops below the dissociation pressure for the hydrate at the reservoir pressure. The gas flows immediately to the free gas zone.
2. Hydrate decomposition is proportional to depressurization rate, and follows a first order kinetic model.
3. Rock and water expansion during gas production are negligible.
4. The model neglects heat transfer between reservoir and surroundings.
5. The reservoir is produced from a single well located at the center.

3.3.2 Mathematical Background

A simple production model based on depressurization was set up to estimate the production rates from the hydrate reservoir. The model considers the reservoir as a rectangular tank of area *A* and thickness *h*, in which both hydrates and free gas are in contact.

So, the reservoir is just a vessel tank in which both hydrates and free gas are contained, and production is controlled by mass transfer. The mathematical development of the model is based on the assumption that, for a closed system, the total volumetric change must be zero:

$$\Delta V_H + \Delta V_G + \Delta V_W = 0 \qquad (1.5)$$

Where ΔV_i corresponds to volumetric changes in the hydrate zone, free gas zone and water, respectively.
By using mass balance principles it is found that:

$$\Delta V_H = (G_{Hi} - G_{Hr})B_{gH} = A\phi(1-S_{Wi})\Delta h_H \qquad (1.6)$$

$$\Delta V_g = G_{fi}\,(B_{gi} - B_g) + (G_p - G_{eH})B_g \qquad (1.7)$$

$$\Delta V_W = (W_p - W_{eH})B_W = A\phi h_g(S_{Wi} - S_W) \qquad (1.8)$$

G_{Hi}, G_{Hr} = initial and remaining gas in the form of hydrate
B_{gH} = reservoir hydrate volumetric factor
ϕ = reservoir porosity
S_{Wi} = initial water saturation
Δh_H = change in hydrate zone thickness
G_{fi}, G_p, G_{eH} = initial free gas, total gas production and gas produced from hydrate

[13] Khataniar, S.; V.A. Kamath; S.D. Omenihu; S.L. Patil and A.Y. Dandekar. "Modelling and Economic Analysis of Gas Production from Hydrates by Depressurization Method. The Canadian Journal of Chemical Engineering, Volume 80, February 2002

B_{gi}, B_g = reservoir gas volumetric factor
W_p, W_{eH} = total water production and water produced from hydrate dissociation.
h_g = gas zone thickness

The gas influx from the hydrate zone is modeled using Kim's model:

$$\frac{dG_{eH}}{dt} = k_0 A\phi \, e^{-\frac{E}{RT}} (P_{eq} - P) \tag{1.9}$$

where P_{eq}, the dissociation pressure, is a function of the reservoir temperature[14]:

$$log_{10}P_D = 0.0342(T_D - 273.15) + 0.0005(T_D - 273.15)^2 + 6.4804 \tag{1.10}$$

The gas production is modeled by the standard backpressure equation:

$$Q_g = C\,(P^2 - P_w^2)^{0.5} \tag{1.11}$$

Where C is the well deliverability constant and P_w is the bottom hole well pressure. For a user-specified pressure profile and assuming adequate C values, the gas production as a function of pressure can be calculated. Then, if we know how pressure changes with time, the production as a function of time can also be estimated. This is done by using the approximation:

$$\frac{dP}{dt} = \frac{P_{n+1} - P_n}{t_{n+1} - t_n} \tag{1.12}$$

Then, the time t_{n+1} corresponding to the pressure P_{n+1} is:

$$t_{n+1} = t_n + \frac{P_{n+1} - P_n}{dP/dt} \tag{1.13}$$

The pressure derivative respect to time is obtained from material balance equation as:

$$\frac{dP}{dt} = \frac{\left[Q_g B_g \left\{ 1 + \frac{k_w \mu_g}{k_g \mu_w} \right\} - \left\{ B_g - B_{gH} + 8.33 \times 10^{-4} B_w \right\} \frac{dG_{eH}}{dt} \right]}{\left[A\phi(1 - S_{wi}) \frac{h_g}{B_g} \frac{dB_g}{dP} \right]} \tag{1.14}$$

In the formulation the model set up is simple:

[14] Ji, Chuang, G. Ahamadi, D.H. Smith. "Natural Gas Production from Hydrate Decomposition by Depressurization". Chemical Engineering Science, Volume 56 (2001), pp. 5801 - 5814

1. Assume a pressure profile, for instance from an initial reservoir pressure of 10 MPa to a well bore pressure of 2MPa.
2. Compute all pressure dependent factors in equation (1.14):

$$Q_g = C\,(P^2 - P_w^{\,2})^{0.5} \tag{1.15}$$

$$B_g = \frac{P_{sc} T Z}{T_{sc} Z_{sc} P} \tag{1.16}$$

Z-factor is also pressure-dependent, and can be estimated using the Hall-Yarborough equation[15]:

$$Z = \frac{0.06125 P_{pr} t e^{-1.2(1-t)^2}}{y} \tag{1.17}$$

Where P_{pr} is the pseudo-reduced pressure, $t=T_{pc}/T$, T_{pc} is the pseudo reduced temperature and y, the pseudo-reduced density, can be estimated as the solution of the equation:

(1.18)

$$-0.06125 P_{pr} t\, e^{-1.2(1-t)^2} + \frac{y + y^2 + y^3 - y^4}{(1-y)^3} - (14.76t - 9.76t^2 + 4.58t^3) y^2 + (90.7t - 242.2t^2 + 42.4t^3) y^{(2.18+2.82t)} = 0$$

This is solved by using the Newton-Raphson iterative method.

The derivative of B_g with respect to P is calculated from B_g definition and recognizing pressure-dependence of Z-factor.

$$B_g = \frac{P_{sc} T Z}{T_{sc} Z_{sc} P} \tag{1.19}$$

Differentiating with respect P and applying the chain rule:

$$\frac{dB_g}{dP} = \frac{P_{sc} T}{T_{sc} Z_{sc}} \left[Z \frac{d(1/P)}{dP} + \left(\frac{1}{P} \right) \frac{dZ}{dP} \right] \tag{1.20}$$

As the pseudo-reduced pressure is $P_{pr}=P/P_{pc}$, where P_{pc} is the critical pressure, Z-factor is:

$$Z = \frac{0.06125 P t e^{-1.2(1-t)^2}}{y P_{pc}} \tag{1.21}$$

[15] Dake, L.P. Fundamentals of Reservoir Engineering. Elsevier Scientific Publishing Company, New York 1978. p.19

Neglecting pressure dependence of pseudo-density:

$$\frac{dZ}{dP} = \frac{0.06125t\,e^{-1.2(1-t)^2}}{yP_{pc}} \tag{1.22}$$

Then, substituting equation (15) in equation (13) and differentiating:

$$\frac{dB_g}{dP} = \frac{P_{sc}T}{T_{sc}Z_{sc}}\left[-\frac{Z}{P^2} + \frac{1}{P}\left(\frac{0.06125t\,e^{-1.2(1-t)^2}}{yP_{pc}}\right)\right] \tag{1.23}$$

This equation completes the set of equations needed for the model setup. The model was programmed using MATLAB® (code shown in Appendix) for a range of pressures and adequate reservoir parameters.

3.3.3 Model Results

In order to estimate gas production rates from the reservoir it is necessary to choose adequate parameters for the model. The main constraints are as follows:

1. Total recovery (both from hydrate and free gas) = 50%.
   Cumulative production from hydrate zone = $7x10^9$ cubic feet
   Cumulative production from free gas zone = $2x10^9$ cubic feet
2. Well deliverability to meet this condition = 0.00026 SCM/s-Kappa
3. Initial Reservoir Pressure = 10,000 Kappa
4. Bottom hole Well Pressure = 2,000 Kappa
5. Water Saturation
   Free Gas Zone = 85%
   Hydrate Zone = 10%
6. Reservoir Porosity
   Free Gas Zone = 4%
   Hydrate Zone = 20%
7. Reservoir Temperature = 10ºC

Note that these values might not correspond to the actual experimental data for the Hydrate Ridge field, but are used instead to back calculate the gas hydrate production (free gas/hydrate). In fact, it was thought to use different porosity and saturation values for each zone, as opposed to the original model formulation.

Based on these assumptions and values, the performance of the hydrate reservoir was modeled. Figure 1 shows pressure variation in the reservoir. It can be noted that after the 6^{th} year, no further reduction in pressure occurs, which means stabilized gas production.

Figure 2 how the cumulative production from the hydrate zone, the free gas zone and the total cumulative production change over time. It can be seen that the 50% recovery target

is reached in about 7 – 8 years. Total cumulative production would be around 10 billion cubic feet, which correspond to 7 billion produced from hydrate zone plus 3 billion cubic feet produced from the free gas zone. Interesting to note that hydrate dissociation does not begin until the first year of production has been reached, which correspond to the point where reservoir pressure falls below dissociation pressure for the hydrate. Figure 3 shows the production rates that could be achieved if the pressure drop and reservoir conditions are reproduced by this model. Initial production rates are in the order of 8 million cubic feet per day (MMCFD), which drop very quickly as free gas zone is depleted. By the 4th year, free gas is completely produced, and gas production is due totally to the hydrate (Figure 4).Gas production is stabilized around 3 MMSCFD.

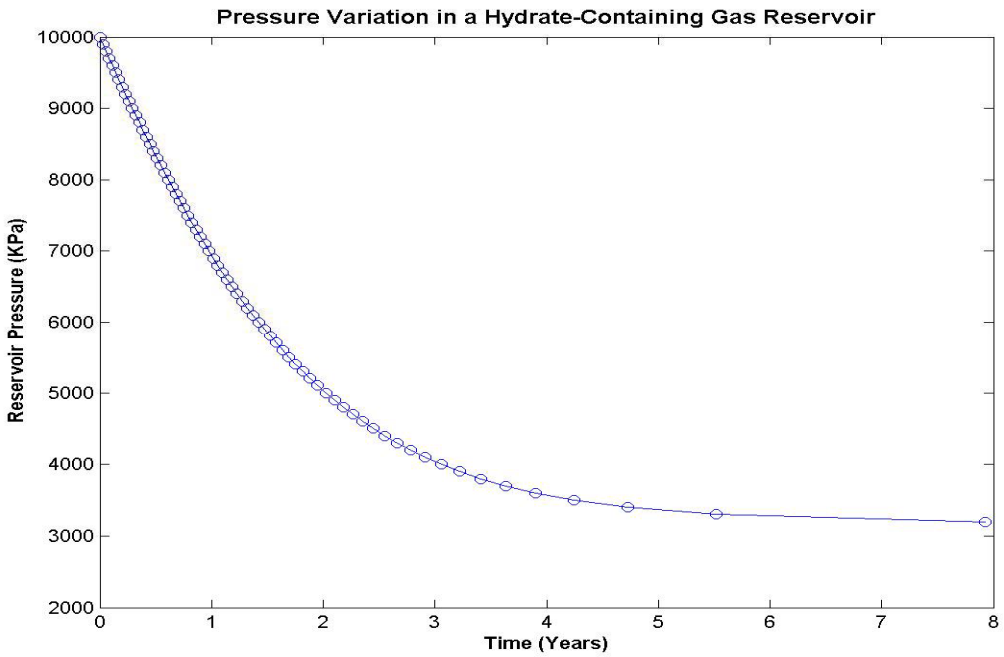

Figure 1: Pressure Variation in the reservoir

Under this "tank model", a hydrate thickness variation can be calculated from the dissociation rate equation as:

$$\frac{dh_H}{dt} = k_0 \, \mathrm{e}^{-\mathrm{E/RT}} (P_{eq} - P) \frac{B_{gH}}{(1 - S_w)} \tag{1.24}$$

Then, the thickness for any time t is calculated as:

$$h(t) = h_0 + \frac{dh_H}{dt}(t - t_0) \tag{1.25}$$

Figure 5 shows the results. As expected, hydrate zone thickness does not change during the first year as reservoir pressure is over dissociation pressure. By the end of production period, thickness would have been reduced about 50%, as expected by the recovery limit set.

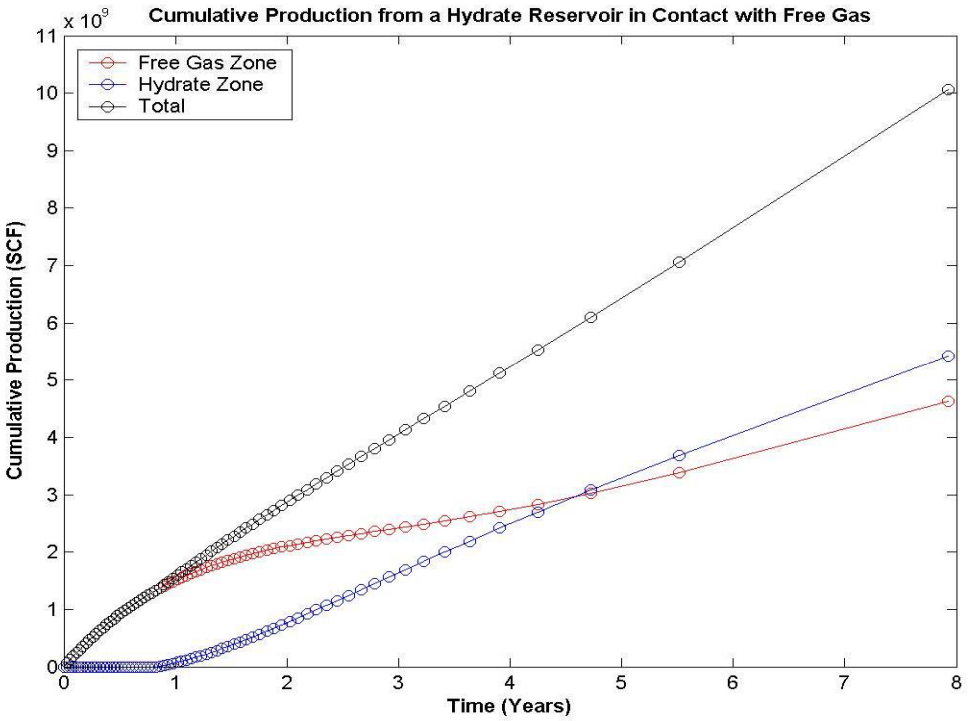

Figure 2: Cumulative production from the reservoir

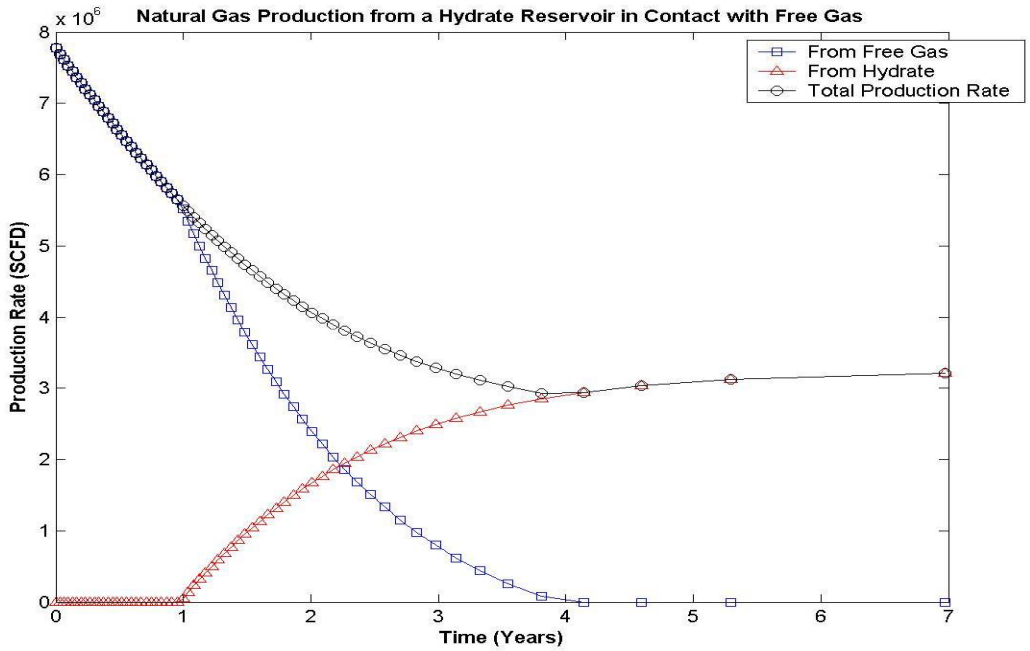

Figure 3 : Natural Gas Production from the reservoir

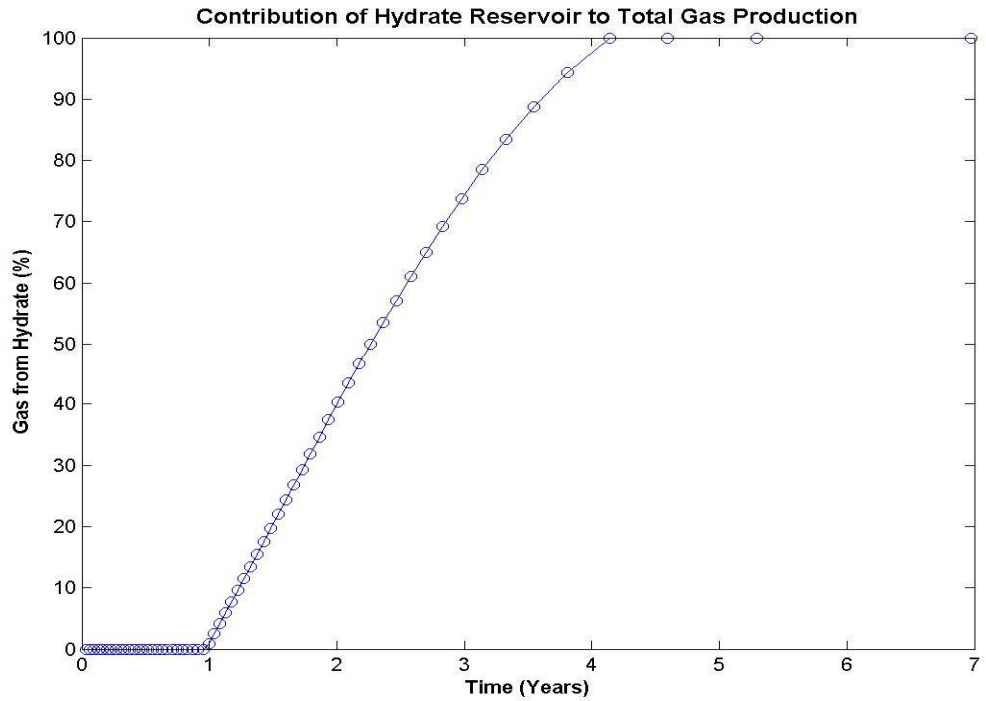

Figure 4: Contribution of Hydrate Reservoir to Total Gas Production

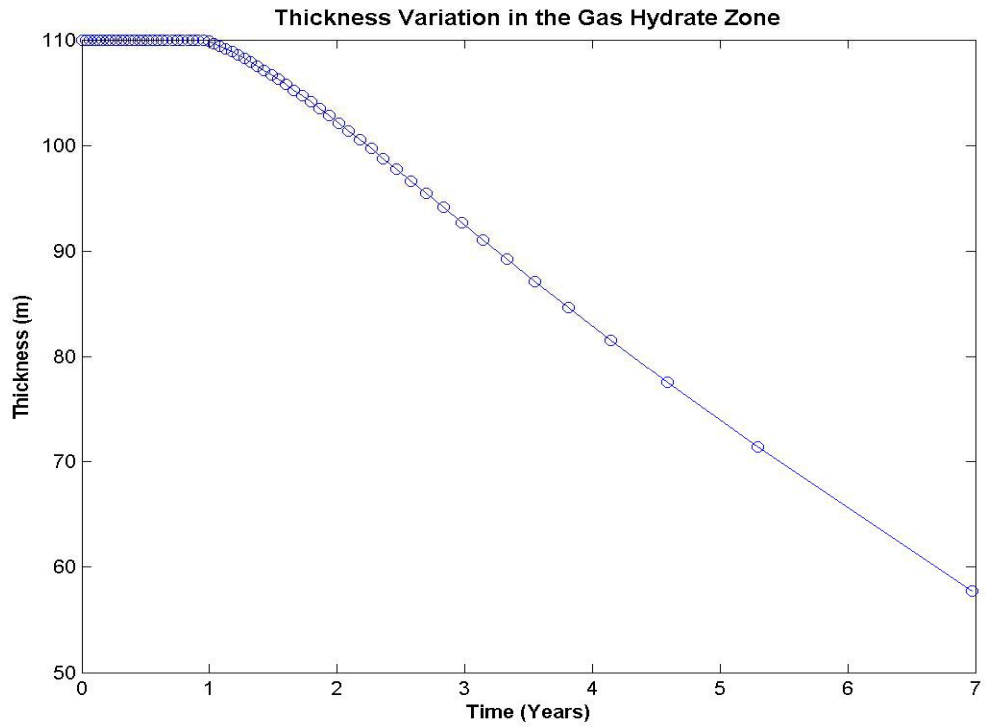

Figure 5: Thickness Variation in the Gas Hydrate Zone

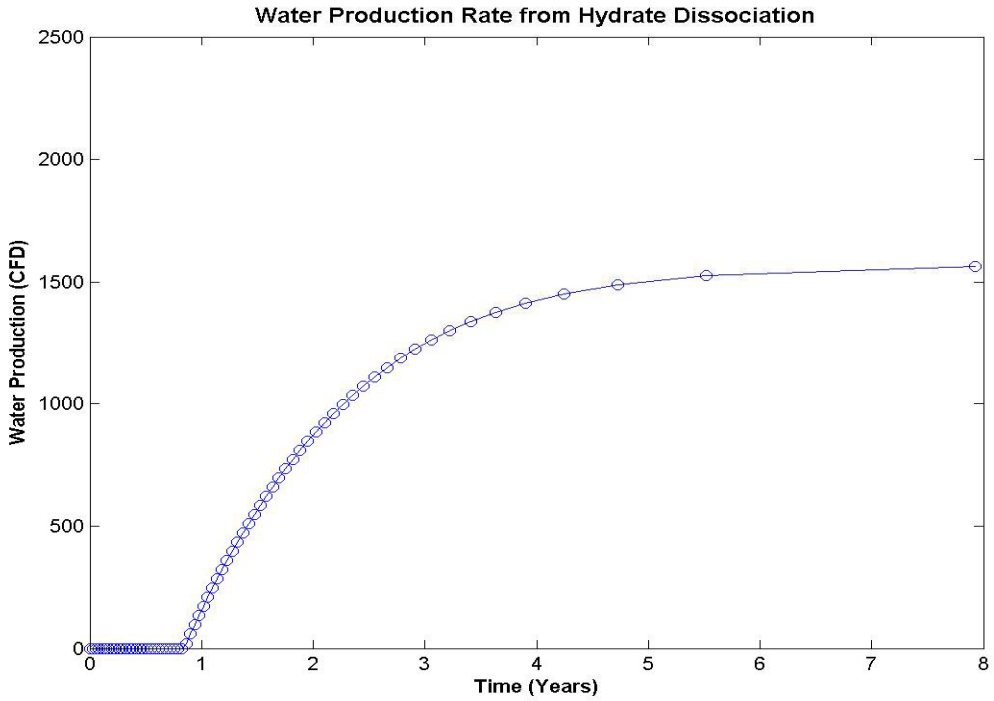

Figure 6: Water Production from Hydrate Dissociation

Water Production can also be calculated using the mass balance as

$$Q_W = \frac{k_w \mu_g B_g}{k_g \mu_w B_w} Q_{gH} \tag{1.26}$$

Where Q_{gH} correspond to gas production from hydrate reservoir. As seen in Figure 6is the water production rate low because of low water saturations assumed? For designing purposes, this means that water handling facilities are not as big as thought they had to be.

The most important output from the model is the cumulative production values during the project life (7 years), which are going to be used for the economic analysis.

3.4 Slope Stability Analysis for Gas Hydrate Production

3.4.1 Assumptions

1. The infinite plane theory applies (1-dimension = depth).
2. Factor of safety can be calculated with respect to depth (dF_S/dz is a linear solution.).
3. The dissociation of gas hydrate is linear with respect to depth.
4. The strength of gas hydrate bearing sediments is greater than that of underlying sediments in the free gas plane before production starts[16]

3.4.2 Strength Properties

The strength parameters for sediment containing gas hydrate in pores is crucial to evaluating the slope stability for a given site. Frozen sediments are affected by a number of factors including strain rate, temperature, consolidation stress, grain size, and density. Factors such as cage occupancy are also believed to contribute to strength of sediments containing gas hydrates[16].

Winters et al.[16] tested samples containing natural gas hydrate from field samples, field samples without gas hydrate, and laboratory formed samples consisting of sieved Ottawa sand (SOS). The SOS samples were tested under conditions of water-saturated, frozen (ice from water), and with gas hydrate formed in laboratory. The strength parameters obtained from this analysis can be found in appendix.

These strength properties have been analyzed to create a graphical relationship between shear stress and axial strain. These curves allow for determination that cementation is a significant factor in the strength properties of the samples. The observations show that gas hydrate SOS was stronger than field sample with gas hydrate. The field sample containing gas hydrate was stronger than similar samples not containing gas hydrates. The sample with the highest maximum shear strength was the sample of frozen SOS, although the laboratory-created SOS with gas hydrate has a higher Young's modulus [16].

3.4.3 Stability Analysis (adapted from Stability of Soil Masses in Cold Regions)

The approach to stability analysis depends on strength properties such as effective angle of friction and effective cohesion, which can be obtain from Figures A and B in the appendix and calculation. The analysis considers stability factors depth (relative to seafloor and the BSR), angle of slope at site, effective sediment and water unit weights, and excess pore pressure in the bearing sediment of the gas hydrate stability and free gas zones. The method used in 8.2 of Andersland and Labanyi's Frozen Ground Engineering was modified to model the stability at the summit of Southern hydrate ridge.

3.4.4 *Factor of Safety*

$$\text{Factor of Safety} = \frac{c + (d\gamma_s(\cos^2 i) - p_f)\tan\phi}{d\gamma_s \sin i \cos i} \qquad (1.27)$$

Where c is cohesion, d is depth below sea floor, γ_s is the unit density of the sediment, i am the slope angle at the failure surface of the slip planes, and Φ is the angle of friction.

[16] Winters, W.J., Pecher, I.A., Waite, W.F., and Mason, D.H. (2004) Physical properties of rock physics models of sediment containing natural and laboratory-formed methane gas hydrate. American Geologist, vol 89, pp. 1221-1227

Factor of safety reflects the balance between stabilizing and destabilizing forces, if it goes less than 1, the formation is likely to fail. Depths to consider (1.27) in would be the seafloor (d = 0) and the base of the concentrated gas hydrate (d ~ 40 m) and the depth of the BSR (~ 110 m). The upper and lower limits of the strength parameters, density of sediment, angle of friction, and slope angle can all be attained from works cited above in the above section.

3.4.5 Conclusions of Stability Analysis

As d decreases, it can be seen from (1.27) that the Factor of Safety increases, the pressure p_f decreases continually as the reservoir is being depressurized. So, the factor of safety will only increase over time provided no external fluid is enters the formation. Hence, we feel that subject to the above assumptions, production is not affected by slope stability.

4 Utilization

4.1 Methanol Synthesis

4.1.1 Why choosing methanol as conversion product

Based on the comparison of the revenues and costs of different conventional technologies we chose methanol synthesis from natural gas reforming as the downstream process. Process parameters, capital requirements and the potential to enhance cash margins are the primary focus of the analysis. Gas-to-Liquid (GTL) technology is a technology to converts natural gas into a high value synthetic liquid hydrocarbon. This technology can be used to reduce gas transportation cost, helps satisfy the demand for cleaner fuels, and fetches higher revenues. This technology is a two step process, synthesis gas formation from natural gas, followed by synthetic liquid fuel formation.

4.1.2 Main Reactions Involved in Synthesis-Gas Production

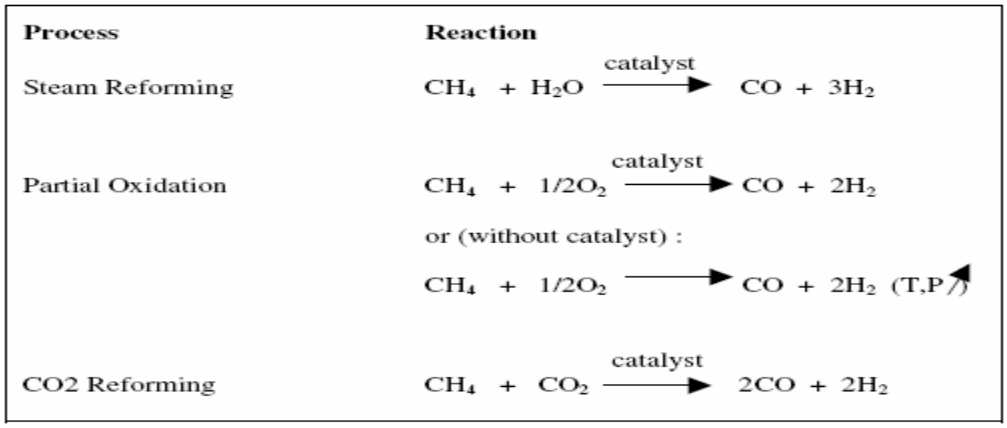

Fig 2. Reactions of synthesis gas formation

Figure 7: Reactions in Methanol Synthesis Ref.

1. Steam reforming[17]:
$CH_4 + H_2O \rightarrow CO + 3H_2$ $\Delta H_r = +206$ kJ/mol, catalyst (1.28)

2. Partial Oxidation: (1.29)
$CH_4 + 1/2O_2 \rightarrow CO + 2H_2$ $\Delta H_r = -35.65$ kJ/mol, catalyst
$CH_4 + 1/2O_2 + N_2 \rightarrow CO + 2H_2 + N_2$ $\Delta H_r = -35.65$ kJ/mol, catalyst

Although currently steam reforming of natural gas is the largest source of all the industrially generated 'reforming products' for our study we have chosen Catalytic Partial Oxidation (CPO) of natural gas to produce synthesis gas. The biggest advantage of this process is the replacement of the highly endothermic steam reforming process by the exothermic partial oxidation process. Given below is an outline of the steps involved in Partial Oxidation (POX).

The fuel is introduced into the reactor with a controlled amount of oxygen. The oxidation reaction is highly exothermic and reaction rates are generally very rapid. For the oxidant we can either use pure oxygen or air depending on process & end-use requirements[18]. For methanol synthesis, the ideal H_2/CO ratio is 2/1. This is best described by the so-called stoichiometric number (SN)[19]:

$SN = (n_{H2} - n_{CO2}) / (n_{CO} + n_{CO2})$

Steam reforming of natural gas yields a synthesis gas with SN number of approx. 3, whereas partial oxidation of natural gas produces synthesis gas with a SN =2 , which is the preferred ratio for methanol synthesis.

[17] Arianto, I. D., "Converting gas into liquid fuels to develop RCD Field, central sumatera, Indonesia, SPE 64708.

[18] Docter, A.; Lamm, A. Gasoline fuel cell systems. J Power Sources, **1999**, 84 (2), 194-200.

[19] Supp, E., "Improved methanol production and coversion technologies".Energy Prog, 1995,5(3), 127-130.

4.1.3 Process Flow sheet

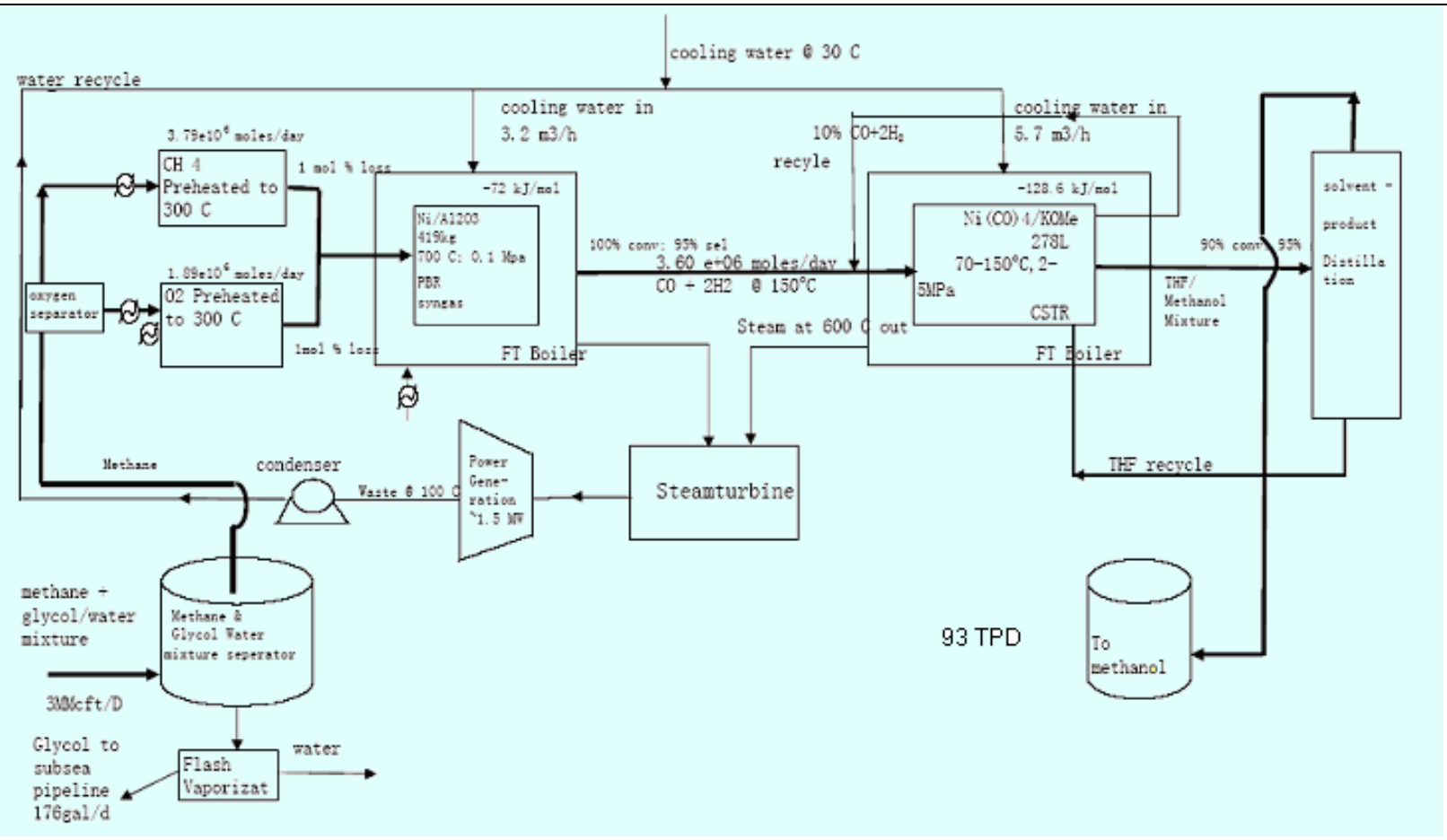

Figure 8: Process Flow sheet- Methanol Synthesis

4.1.4 Assumptions

1. 100% conversion and 95% selectivity are assumed.
2. Methane and oxygen preheated to 300°C.
3. The steam reforming take place at 700°C.
4. The reactor is adiabatic.
5. The CH_4/O_2 ratio = 2:1.
6. No carbon dioxide is produced during syngas synthesis.
7. GHSV/ (h^{-1}) based on the reaction kinetic of 700°C is 1.40*10^5
8. The reaction is operated under low temperature and medium pressure.
9. Space time yield of catalyst (g-mol MeOH/ kg Cat. H) = 570.
10. Homogeneous catalysis reaction.
11. The catalyst Nickel tetra-carbonyl $Ni(CO)_4$ (0.05M) activated by an alkoxide base KOMe) (0.1M) in a THF solvent.

12. The total catalyst volume required is 278 liter.

4.1.5 Catalyst Selection for Reforming

The catalyst selection in both steps was based on the consideration of different parameters, such as operating temperature, catalyst activity, conversion % and selectivity & price.

Partial Oxidation Catalyst: The catalyst chosen was Ni (2.5 wt %) catalyst on Al_2O_3 support[20]. Nickel shows good activity for hydrogen transfer and is commonly used in stationary plants for hydrogen production by both partial oxidation and steam reforming. The reforming reactor is a packed bed type. The reaction conditions are 500 °C and 1atm; Residence time is 0.1s; Catalyst selectivity with respect to CO is 95% & conversion efficiency is 100%.[21]

Syngas to Methanol conversion: The homogeneous catalyst system chosen for this step comprises of a nickel complex, Nickel tetra-carbonyl $Ni(CO)_4$ (0.05M) activated by an alkoxide base (KOMe) (0.1M) in a THF solvent. This novel catalyst system produces methanol from natural gas-derived synthesis gas at a lower temperature of <150°C and <5 MPa pressure with high selectivity (>95%) and high productivity and achieves >90% per pass syngas conversion thus lowering the number of for a gas recycles. The reaction constant is a pseudo first order rate constant. Based on experimental data k was calculated to be 0.083 min^{-1} and c = 6.26. Similarly k and c values for H2 were calculated to be 0.035 min^{-1} and 0.991 respectively[21]. The dependence of k on MeoH concentration is given by the equation $k = k_1 exp(k_2[MeOH]$ where k_1 and k_2 are 1.71 min^{-1} and 0.443 M^{-1}

4.1.6 Economics Analysis of Methanol Production

The economic analysis examines the cost of each process according to the natural gas throughput and product rates. Required capital investment for a conventional methanol production facility of ~ 100 metric tons/day = $ 10 million. The major factors affecting this capital cost include: Steam costs, methanol synthesis, distillation, utilities, offsites, oxygen unit & glycol separation.

The break-up of these costs is given in Appendix B. The methane production rate from site 1249 is about 3 million cft/d. Based on this value and total recoverable reserves, the fixed costs were evaluated to be ~ $ 1.5 million. The operating costs are assumed to be around 7.5% of capital costs[22]. Adding this to the transportation cost for methanol, we get the annual average cost of a methanol production plant of above

[20] Zaman, J., "Oxidative process in natural gas conversion", Fuel Processing Technology, 1999, 58, 61-81.

[21] James E. Wegrzyn, Devinder Mahajan, Michael Gurevich "Catalytic routes to transportation fuels utilizing natural gas hydrates", Catalysis Today 50 (1999) 97-108.

[22] Seddon D., "Technology and Economics o Gas Utilization: Methanol", SPE 28790, **1994**, 473-484.

capacity as $ 0.27/gal methanol produced. This cost estimate involves only the downstream processing cost. The average cost of methanol production including upstream and downstream operations in the Hydrate Ridge site 1249 is given in subsequent sections. The combined heat of reaction from the partial oxidation step and methanol production step can be used to generate ~ 1.5 MW of power. This can be used to power all the upstream and downstream operations during methane hydrate recovery & utilization.

4.2 Hydrate Slurry Process

4.2.1 Why hydrate slurry process:

The cost of a floating production platform with offloading facility is estimated to be ~112 million $[23]. From our discussions with Dr. Robert Watson, a higher figure of 200 million $ was found[11]. A lesser capital intensive method for producing methane from hydrates would be the use of a subsea system where hydrates are formed at the seafloor, slurried with water and transported in a pipeline back to shore. The costs involved in such an operation are given in the following paragraphs. Although similar systems have been proposed, they rely on a surface floating vessel to store/carry the hydrate[24]. Also, the proposed heat exchange mechanism in Ref. is different from that proposed here.

4.2.2 Introduction:

A sketch of the process is as shown in Figure 9. Natural gas produced by depressurization (or other techniques) is collected by a subsea system which feeds the gas to a few heavy duty compressors/multiphase pumps where it is compressed from 2 MPa to 6 MPa. It is cooled to the seawater temperature using a heat exchanger. It is then passed to stainless steel water jacketed tanks (which are a part of the subsea template). The gas from the compressor/multiphase pump is cooled with sea water to ~6°C (using preferably a plate heat exchanger). Details of the compression and heat exchange calculations can be found in the Appendix **Error! Reference source not found.**. The hot sea water might be used to supply energy to decompose hydrates (plugging the tanks). As the gas is sparged through the sea water, the pressure in the tank continuously rises until gas hydrate formation occurs. The stirrer breaks up aggregates of gas hydrates into smaller particles. The power consumption for stirring is taken to be 10 HP/1000 gal[25]. Though this work does not consider the kinetics of gas hydrate formation, a residence time of 1 hr in the reactor (based on slurry volume) is considered enough for the formation of hydrates (resulting in a reactor volume of 72 m^3.) After the desired set point pressure in the tank has been reached, the gas flow is cutoff and is diverted to the empty tanks. Excess gas content in the slurry might be removed by means of a gas-slurry separator.

[23] http://tonto.eia.doe.gov/FTPROOT/modeldoc/m063(2001).pdf

[24] Waycuilis J.J, York S.D., United States Patent US 6703534 B2, Transport of Wet Gas Through a Subsea pipeline, Mar. 9, 2004., Marathon Oil Company, Findlay, OH, U.S.

[25] http://www.clarkson.edu/~wilcox/Design/heurist.pdf

The water concentration in the slurry is maintained at ~32 % as it was found that 32% suspensions of gas hydrates in water have the same viscosity as pure water at 4° C[26].

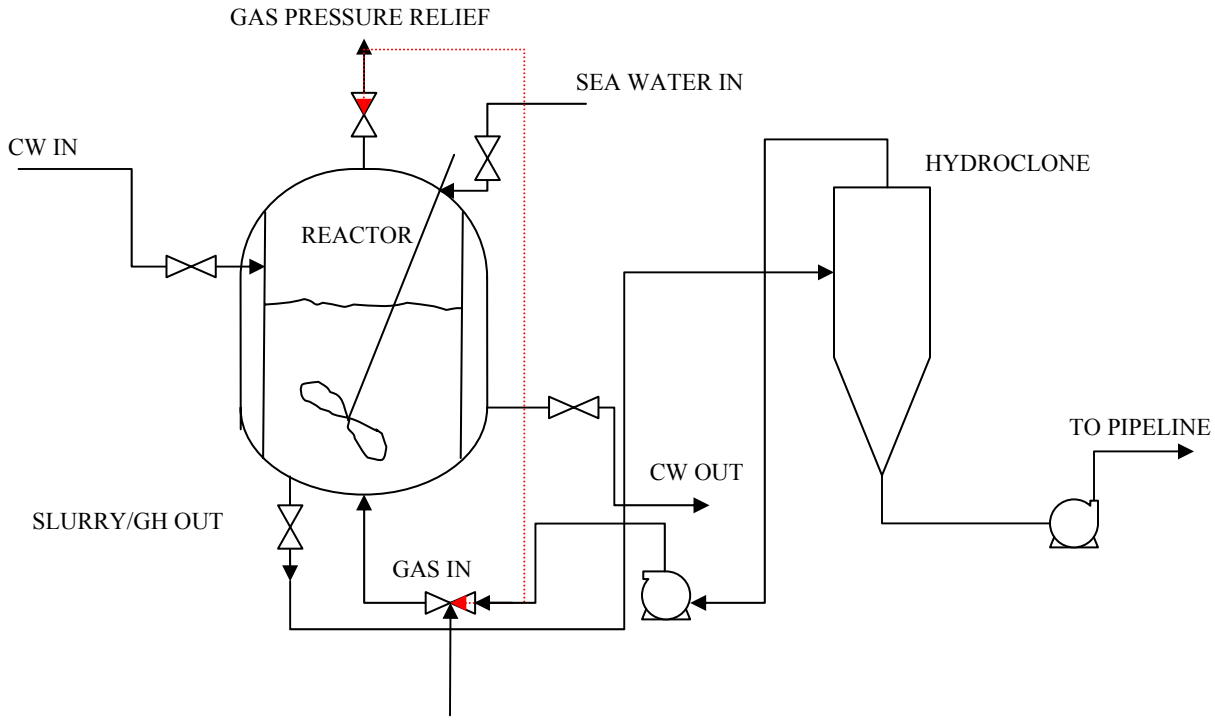

Figure 9 : Hydrate Slurry Process Flow Diagram

4.2.3 Assumptions :

1. Natural gas from the production well is assumed to be at a pressure of 2 MPa, 4°C.
2. A constant production rate of 3 million cubic foot/day is assumed.
3. The topside control equipment are located on the shore with communicating with the site by a fiber optic cable and electrical power line. Costs for building a control station are assumed to be small when compared to other costs (like pipeline cost), while the costs of a subsea electrical line are accounted for.
4. The subsea templates are located in regions of low hydrate concentration; i.e. the sediment supporting the subsea template(s) is assumed to be stable. (Typical subsea modules weigh 65 MT with the Christmas tree, valve, choke, isolation, controls, pigging cross over, pipeline and trunking and flowline connection modules[27])
5. The cost of a glycol pipeline is ~ 0.5 times that of the slurry pipeline.
6. The number of wells connected to a subsea template is taken to be 8[28].

[26] Gudmundsson J S, Cold Flow Hydrate Technology, 4th International Conference on Gas Hydrates, May 19-23, 2002, Yokohama, Japan.
[27] Goodfellow Associates, Applications of Subsea Systems, pg: 65, Pennwell Books, 1990.
[28] Goodfellow Associates, Applications of Subsea Systems, pg: 62, Pennwell Books, 1990.

7. A Work Class Remotely Operated Vehicle (WROV) operating from a barge is used for well intervention if the need arise. Costs of a WROV (3.5 million $ capital cost) are not accounted for.
8. Pump efficiency is assumed to be 40%.
9. Capital cost of pipeline is $80000 /in-mile[29]. From our discussions with Dr. Watson[11], a 12" pipeline would cost $1 million/mile (which is roughly the same as the value stated.)
10. Costs of heat exchangers are not accounted for.
11. This analysis does not consider the kinetics of hydrate formation. Hydrate formation was described by a gas bubble to hydrate crystal model by Morti and Gudmundsson[30]. The formation rate was found to be sensitive to the methane injection rate and pressure inside the reactor.

4.2.4 Comparative Economic Analysis of Hydrate Slurry and Methanol Conversion*:*

Figure 10 gives an estimate of the pipeline capital and operating costs for various pipe diameters. The capital costs of pumps were not considered in the analysis. Operating costs comprise costs due to pumping slurry (viscosity similar to water) over 100 km. As mentioned earlier a gas hydrate concentration of 32% was used. The capital cost of a pipeline is as stated in the assumptions. The calculations also account for the cost of a glycol line. The methodology of pipeline calculations follows engineering pipe sizing

[29] Team III, Team III Literature Review Report, FSc 503, Fall 2004, Pennsylvania State University.
[30] Mork M., Gudmundsson J.S., Hydrate Formation in a Continuous Stirred Tank Reactor: Experimental Results and Bubble to Crystal Model, 4th International Conference on Gas Hydrates, May 19-23, 2002, Yokohama, Japan.

calculations and is presented in the Appendix: **Error! Reference source not found.**.

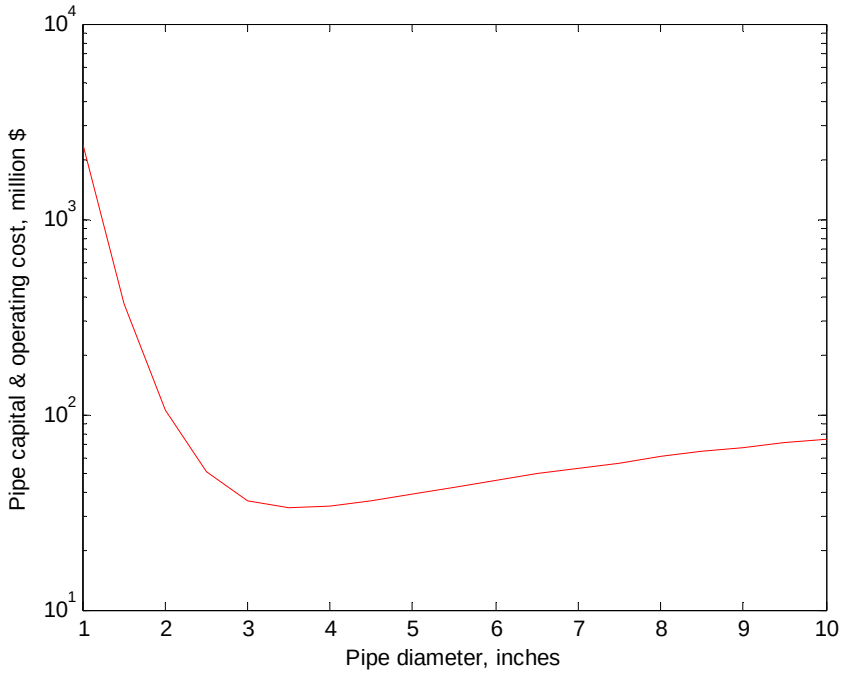

Figure 10 : Pipeline capital and operating costs, million $

Calculation of number of pumps needed: From the Slurry Systems Handbook[31], a centrifugal pump can supply heads of 40 m at 800-1000 gpm flow rates. The flow rate for slurry transport is ~1000 gpm and the total head (for a 4" pipe) is 4716 m. Hence, ~118 pumps are needed to supply the total head. Assuming the cost of a pump to be ~50000 $, the total cost of pumps comes to 5.9 million $.

[31] Abulnaga B.E., Slurry Systems Handbook, McGraw-Hill, 2002, Chapter 8

The capital cost of equipment needed onshore for dissociating hydrates (pumps, heat exchangers, tanks) is taken to be 1 million $. A similar value for the operating costs is assumed.

Hydrate Slurry Case			Base Case		
Production	7665000	MCF	Production	7665000	MCF
Capital	Million $	Average cost $/MCF	Capital	Million $	Average cost $/MCF
Drilling	32.00	4.17	Drilling	32.00	4.17
Subsea Template	10.00	1.30	Subsea Template	10.00	1.30
Tank	0.05	0.01	Methanol plant	10	1.30
Pipeline	29.96	3.91	FPSO	112	14.61
Pumps	6.00	0.78			
Electrical line	5.00	0.65			
Dehydration	0.10	0.01			
Dissociation	1.00	0.13			
Total capital	84.11	10.97	Total capital	164.00	21.40
Operating					
Mixing	0.26	0.03			
Compression	0.16	0.02			
Pumping	4.03	0.53			
Dissociation	2.00	0.26			
Total operating	6.45	0.84	Operating	9.00	1.17
Total	90.56	11.82	Total	173.00	22.57
Revenue/MCF		3.00	Revenue/MCF		9.14
Loss/MCF		8.82	Loss/MCF		13.43

Table 1 : Comparison of capital and operating costs between Hydrate Slurry & FPSO-Methanol production

4.2.5 Comments:

From Table 1, we can conclude that hydrate slurry based production is more economical than methanol synthesis based on a floating production platform subject to the assumptions stated. A detailed Net Present Value analysis is given in the previous pages. Some of the practical problems that have to be resolved in this system are :

1. Flow assurance at low temperatures with gas hydrate slurries – assessing the potential for gas hydrate blockage of pipelines
2. Development of subsea non-fouling heat exchangers; Ref 24 mentions the use of a fluidized bed heat exchanger which has little potential for fouling in subsea environments.
3. Further work can also has to consider the kinetics of gas hydrate formation so that reactor sizing and costing can be done more accurately.

5 Results and Discussion

5.1 Production via depressurization

5.1.1 Economic Model

Economic Analysis of Natural Gas Production from Gas Hydrate Reservoirs

A simple economic model based on Discounted Cash Flow Analysis is used to assess the feasibility of natural gas production and utilization from a hydrate reservoir. Two scenario cases are analyzed: (1) Production of natural gas using FPSO unit and on-board conversion to methanol which is sold to the market and (2) production of natural gas and conversion to a hydrate slurry for transportation, which is then decomposed and sold to the natural gas market.

Table 2 shows the yearly natural gas production from the hydrate reservoir modeled. As stated before, it was assumed a 50% recovery of total reserves, which in this case corresponds to a total project life of seven (7) years.

Table 2: Average Natural Gas Production from a Hydrate Reservoir

Year	Average Daily Production (SCFD)	Average Yearly Production (SCF)
1	6.67E+06	2.44E+09
2	4.82E+06	1.76E+09
3	3.68E+06	1.34E+09
4	3.06E+06	1.12E+09
5	2.99E+06	1.09E+09
6	3.12E+06	1.14E+09
7	3.21E+06	1.17E+09
Average Production	**3.94E+06**	**N.A.**
Total Production	**N.A.**	**1.01E+10**

5.1.2 FPSO Process – Methanol Conversion

The cost elements considered in this design are shown in Table 3. As pointed out, process units were scaled for an average processing capacity of 3 MMSCFD.

Table 3: Cost Elements for FPSO-Methanol Process

Cost Element/Process	Million Dollars ($MM)
Capital Cost	
Drilling	32.00
Subsea Template	10.00
Methanol plant	10.00

FPSO	112.0
Total Capital	**164.0**
Operating Cost ($/MCF)	**0.91**

NG Production: 3.0 MMSCFD

In a Cash Flow Analysis, only actual flows of cash are considered, so, financial costs as depreciation are not considered.

Base Case

The base case considers a methanol price about 0.88 $/gal and an inflation rate of 4%. Discount rate is 10%.

Table 4: Discounted Cash Flow Analysis for FPSO-Methanol Process (Base Case)

	Year 0	Year 1	Year 2	Year 3	Year 4	Year 5	Year 6	Year 7
Natural Gas Production (BCF/y)		2.44	1.76	1.34	1.12	1.09	1.14	1.17
Methanol Production (MMgal/y)		25.3	25.3	25.3	25.3	25.3	25.3	25.3
Methanol Price ($/gal)		0.88	0.90	0.92	0.93	0.95	0.97	0.99
Total Sales ($MM)		22.2	22.7	23.1	23.6	24.1	24.5	25.0
Operating Costs ($MM)		**23.0**	**23.0**	**23.0**	**23.0**	**23.0**	**23.0**	**23.0**
Operating Profit ($MM)		**(0.76)**	**(0.31)**	**0.14**	**0.60**	**1.07**	**(0.76)**	**(0.31)**
Income Tax (30%)		(0.23)	(0.09)	0.04	0.18	0.32	(0.23)	(0.09)
Capital Expense ($MM)	(164.00)							
Net Cash Flow ($MM)	**(164.00)**	**(0.99)**	**(0.41)**	**0.18**	**0.78**	**1.40**	**2.02**	**2.66**
Discount Rate (%)	**10%**							
Net Present Value (%)	**(161.18)**							
Rate of Return (%)	N.A.							

5.1.3 Sensitivity Analysis

Feasibility of the project will depend on several factors. The ones considered here are Discount Rate applied to the project.

5.1.3.1 Discount Rate

At the base case production rate and methanol price, the economics of the FPSO-Methanol process are not favorable even considering a discount rate of 0%.

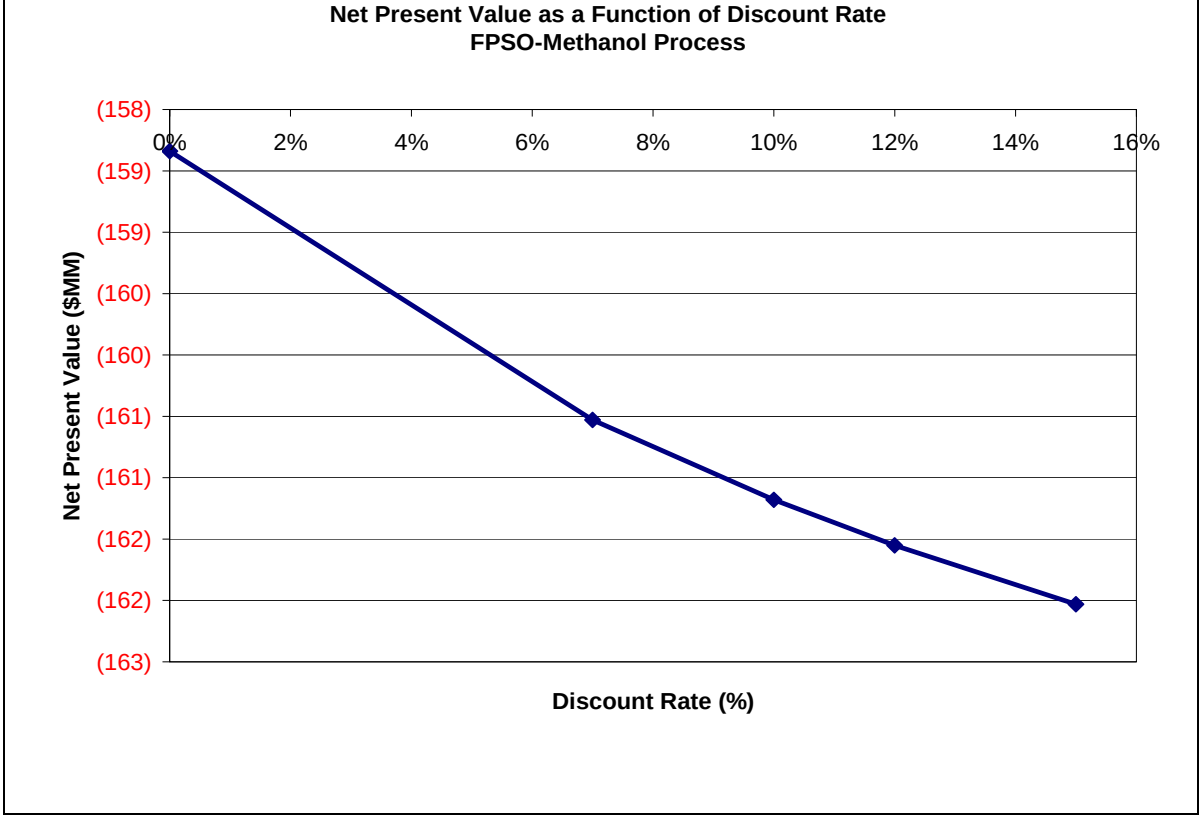

Figure 11: Net Present Value as a Function of Discount Rate

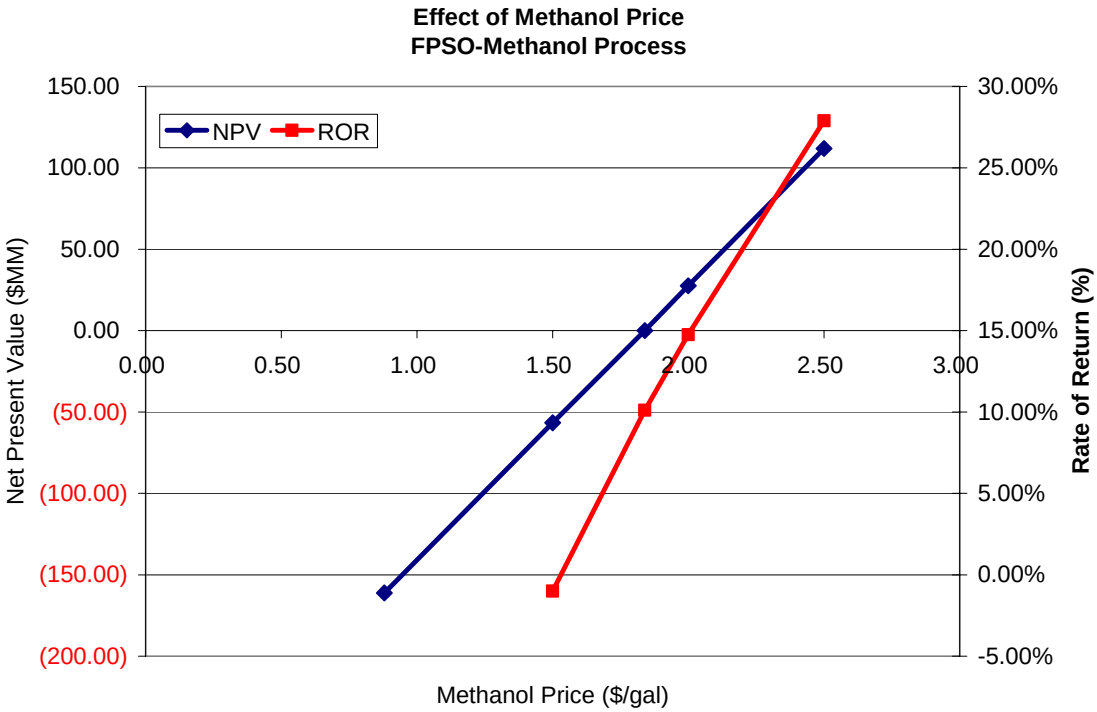

Figure 12: Effect of Methanol Price on Economics

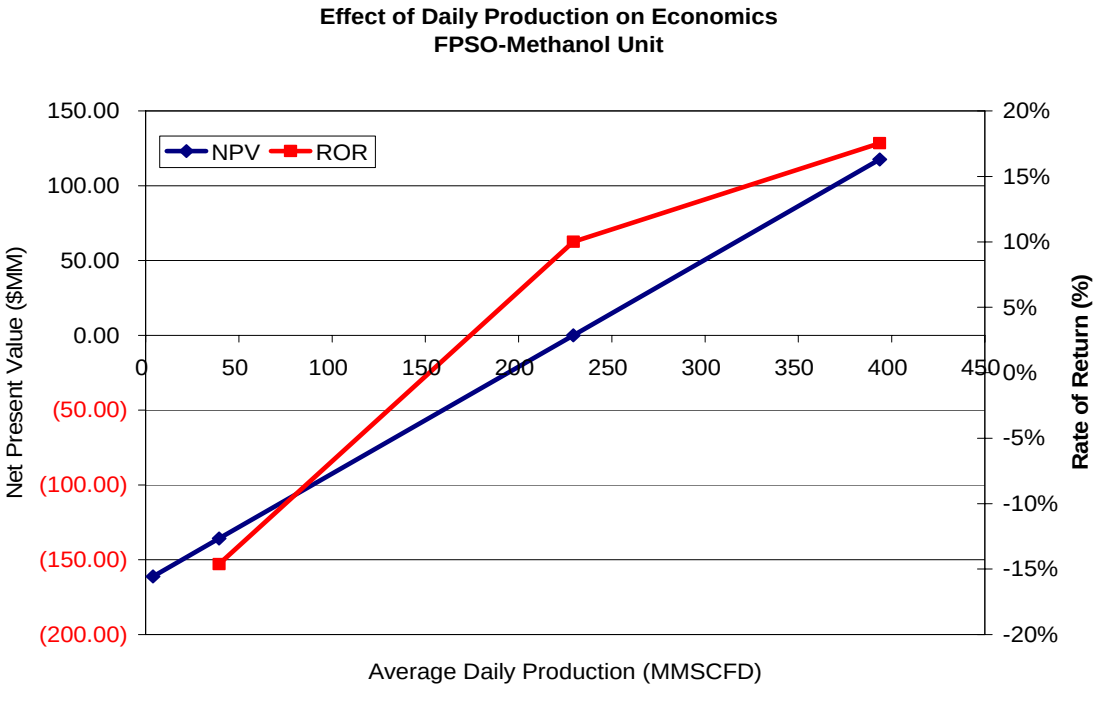

Figure 13: Effect of Gas Production on Economics

5.1.3.2 Methanol Price

The price of methanol seems to be the factor of highest importance for the FPSO process economics. Note that at values of 1.84 $/gal or higher (breakeven), the NPV start to be positive.

5.1.3.3 Average Gas Production

The economics are not very sensible to average daily production. NPV values start to be positive for production rates of 230 MMSCFD. This is more than 50 times the predicted production rate for the Hydrate Ridge field.

Natural Gas Transportation as Hydrate Slurry

The cost elements are shown in Table 5. The base case considers a wellhead price for natural gas of 5.00 $/MCF, an inflation rate of 4% and discount rate of 10%. The scaling of the process considers gas production rate of 3.0 MMSCFD.

Table 5: Cost Elements for Hydrate Slurry Process

Cost Element/Process	Million Dollars ($MM)
Capital Cost	
Drilling	32.00
Subsea Template	10.00
Tank	0.05
Pipeline	29.96
Pumps	6.00
Electrical line	5.00
Dehydration	0.10
Dissociation	1.00
Total Capital	**84.11**
Operating Cost	
Mixing	0.99
Compression	0.15
Pumping	3.68
Dissociation	0.91
Total Operating ($/MCF)	**5.73**

Table 6: Discounted Cash Flow Analysis for Hydrate Slurry

	Year 0	Year 1	Year 2	Year 3	Year 4	Year 5	Year 6	Year 7
Natural Gas Production (BCF/y)		2.44	1.76	1.34	1.12	1.09	1.14	1.17
Wellhead Price ($/MCF)		5.00	5.20	5.41	5.62	5.85	6.08	6.33
Total Sales ($MM)		**12.18**	**9.15**	**7.26**	**6.29**	**6.37**	**6.93**	**7.42**
Operating Costs ($MM)		**13.96**	**10.08**	**7.69**	**6.41**	**6.24**	**6.53**	**6.72**
Operating Profit ($MM)		**(1.78)**	**(0.93)**	**(0.43)**	**(0.12)**	**0.13**	**0.40**	**0.70**
Income Tax (30%)		(0.53)	(0.28)	(0.13)	(0.04)	0.04	0.12	0.21
Capital Expense ($MM)	(84.11)							
Net Cash Flow ($MM)	**(84.11)**	**(2.31)**	**(1.21)**	**(0.56)**	**(0.15)**	**0.17**	**0.52**	**0.91**
Discount Rate (%)	10.0%							
Net Present Value (%)	**(86.87)**							
Rate of Return (%)	N.A.							

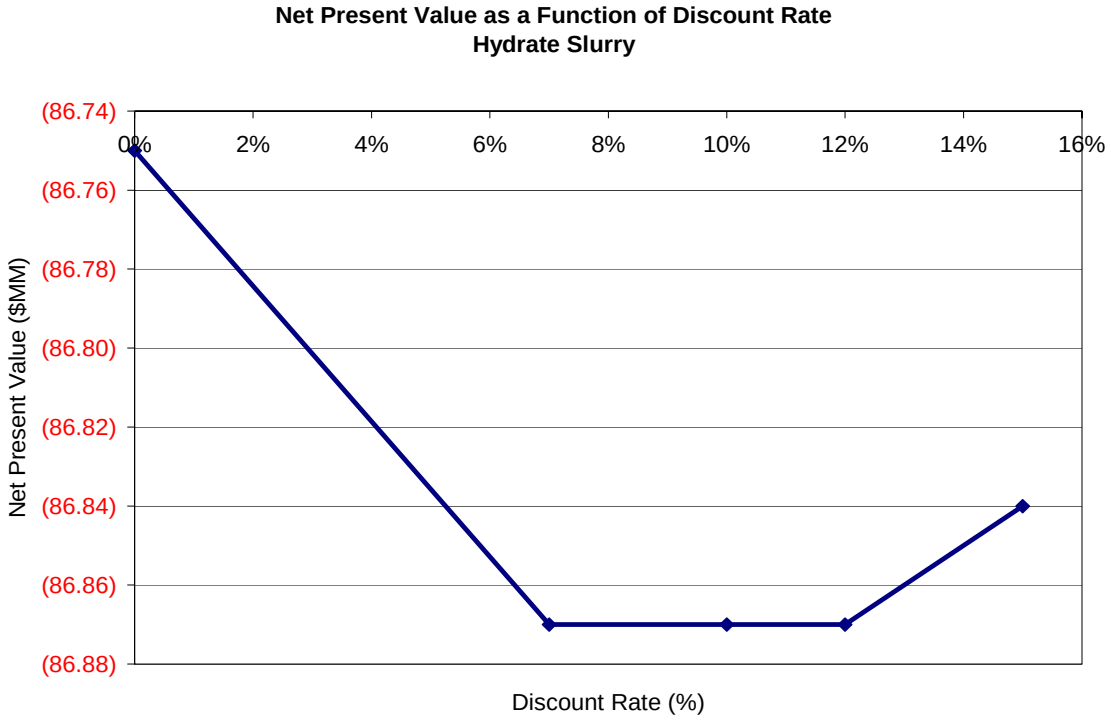

Figure 14: Net Present Value as a Function of Discount Rate

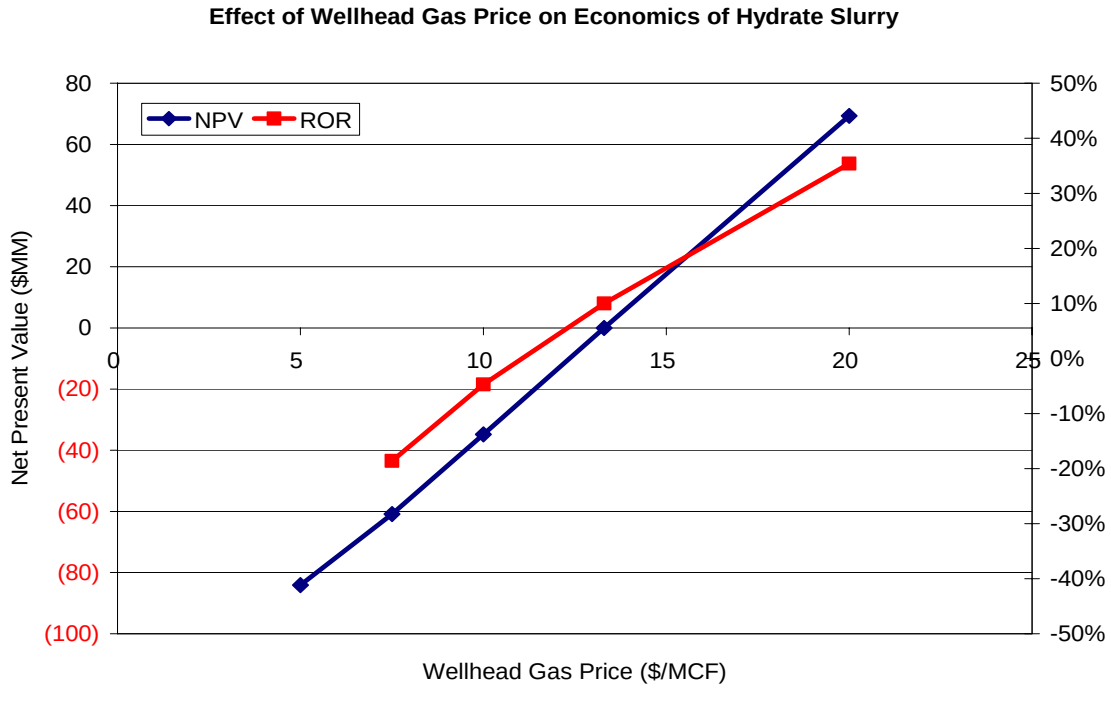

Figure 15: Effect of Wellhead Gas Price on Economics of Hydrate Slurry

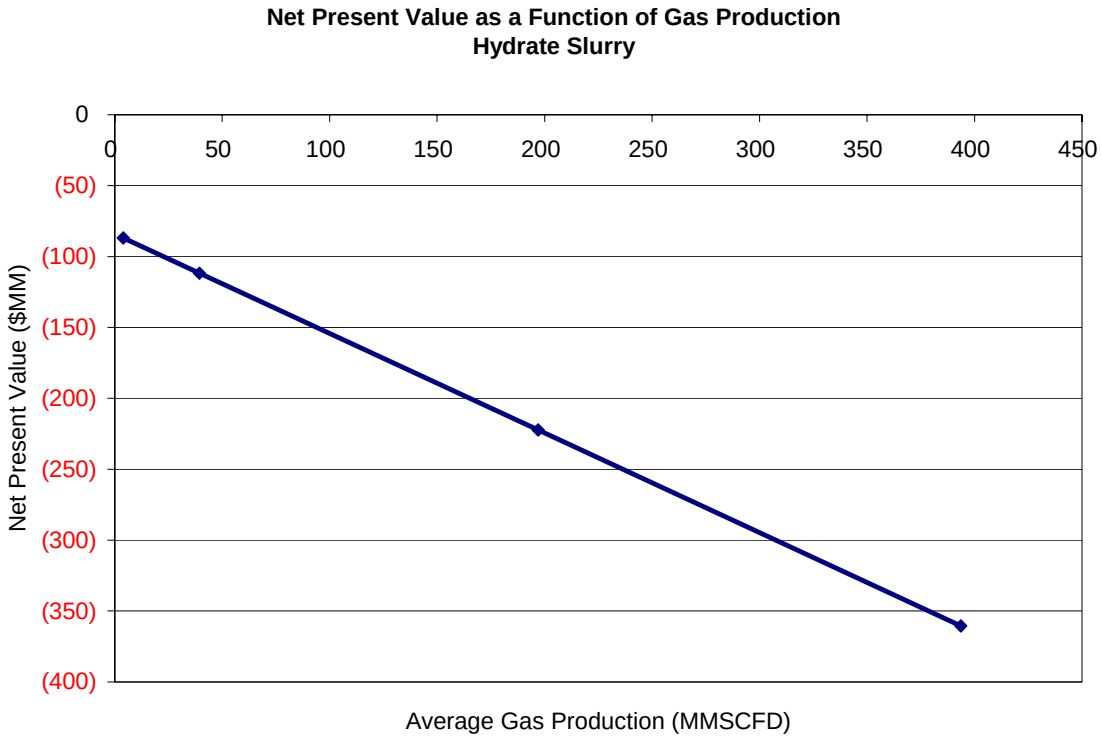

Figure 16: Net Present Value as a Function of Gas Production

Sensitivity Analysis

1. Discount Rate: As for the case for on-board methanol production in a FSPO unit, the discount rate does not have significant effect on net present value.

2. Wellhead Gas Price: This is the most important factor in the analysis. Unfortunately gas prices are expected to fall to values around 4 $/MCF according to the Energy Information Agency[32]. If that is the case, economics of transportation as hydrate slurry will be favored by capital and operational costs reduction.

3. Average Gas Production: Increasing production rates will deter economics for this process given the high operational costs (higher than the wellhead gas price in the base case). Deeper analysis must be performed to assess the economics of the process, especially the operational costs.

[32] Energy Information Administration. Energy Outlook 2004. Document No. DOE/EIA-0383(2004), Washington, D.C., January 2004

5.2 Methanol Synthesis Process Design

5.2.1 Conversion of Methane to Syngas

The process for methanol synthesis is shown in Fig. 1 Natural gas containing glycol/water mixture enters the separation unit. The daily glycol injection rate required for methane production was calculated to be around 176 gal/day. Assuming a glycol recoverability of 90%, maintaining this injection rate costs about $ 30,000/annum. Dehydrated natural gas and oxygen are preheated to 300°C (573°K). The oxygen is produced in an air separation unit. The feed stream is further heated to 700°C in a packed bed reactor (PBR). Here the gas is fed through a catalyst bed of weight 160 kg where it reacts to produce syngas. POX being a highly exothermic process, the reformed gas exits the furnace at 1atm and ~ 1500°C. The heat from the product stream is used to produce steam at 600 °C in a fire tube boiler. A water flow rate of about 3.2 m^3/h is used. This steam is part of the input for the steam turbine generating onboard electricity.

5.2.2 Conversion of Syngas to Methanol

The cooled synthesis gas is then used to synthesize methanol at ~ 150 °C & 5 MPa in a CSTR. A homogeneous catalyst $Ni(CO)_4$/KOMe in a 100% THF solvent whose volume was calculated to be 253 L is used. Again, being a highly exothermic reaction, this step produces about 3.17 X 10^5 MJ/day. This heat is also used to generate steam at 600 °C. This steam is combined with the stream from the syngas step for power generation. The solvent-product mixture is then separated in a distillation unit and the solvent is recycled. The liquid methanol is then shipped to the shore in tankers. The detailed calculations of the heat produced from each reaction and final power generated are shown in Appendix 'B'

5.3 Discussion

5.3.1 Technological Innovations needed for *optimal* recovery

From a Net Present Value perspective, the economics of offshore gas hydrate recovery can be improved if capital costs could be reduced or the rate of recovery could be increased[33]. We feel that the main cost categories are: Drilling, Floating Platform and Utilization/Transportation. In the following section, we present the results of our findings to reduce the capital cost (or) increase the recovery rates from gas hydrate bearing sediments.

5.3.1.1 Cheaper Drilling Techniques

Numerical simulation of production from gas hydrate wells by depressurization was found to result in flow rates of ~500 m^3/d/well [34]. Hence, multiple (~40) wells are needed for gas flow rates which can result in economies of scale. At a drilling cost of 6 million

[33] The idea of Net Present Value analysis is that a dollar at the present is worth more than a dollar after an year.

[34]

$/well, this is economically not justifiable. Cheaper drilling techniques for gas hydrate recovery involving coiled tube drilling and/or low thrust, low torque drilling and have been proposed, though the authors mention that they have been used primarily for vertical wells[35]. In our opinion, most future offshore gas hydrate wells would be directional, not vertical. From our discussions with Dr. Watson**Error! Bookmark not defined.**, we feel that this one of the areas where further research has to be done.

5.3.1.2 Production

5.3.1.2.1 Fraccing

Although we considered different fraccing techniques, it was felt that we did not have enough information on hand to effectively predict the fracture dimensions. As mentioned earlier, an important challenge in fracturing gas hydrate reservoirs is to maintain the higher permeability flow paths near the wellbore. (Fracturing unconsolidated sediments would result in refreezing and plugging of the fracture due to dissociation[36]). Ref also mentions the use of super saturated brine to fracture gas hydrate reservoirs. Time constraints did not allow us to consider this in greater detail.

5.3.1.2.2 Electrical heating

As shown earlier, the rate of dissociation is a thermally limited step. We evaluated the potential for heating the gas hydrate zone by means of passing an alternating current t hrough the wellbore. The assumptions involved in the following analysis are given below:

1. The present analysis describes the electrical heating of a gas hydrate reservoir by means of an electrode placed on the surface of a horizontal well
2. This calculation does not consider a moving boundary condition with phase changes; i.e. heat of dissociation of hydrates is not considered.
3. Convection of gas and water through the gas hydrate and free gas zones is not considered; this might be justified if we consider that the rate limiting step is the heat transfer and not fluid flow.
4. The temperature profile is assumed to be radial
5. The time needed to establish a current flow through the formation is much lesser compared to the timescale of fluid flow and heat transfer.
6. The thermal conductivity of clays with gas hydrate and melted water is almost the same.

[35] Kolle J.J., Max M.D., Seafloor Drilling of the Hydrate Economic Zone for Exploration and Production of Methane, Poster presented at the AAPG Annual Meeting 2002, 2002.

[36] McGuire P.L., Recovery of Gas Hydrate Deposits using Conventional Technology, SPE/DOE 10832, paper presented at the SPE/DOE Unconventional Gas Recovery Symposium of the Society of Petroleum Engineers held in Pittsburgh, PA, May 15-18, 1982.

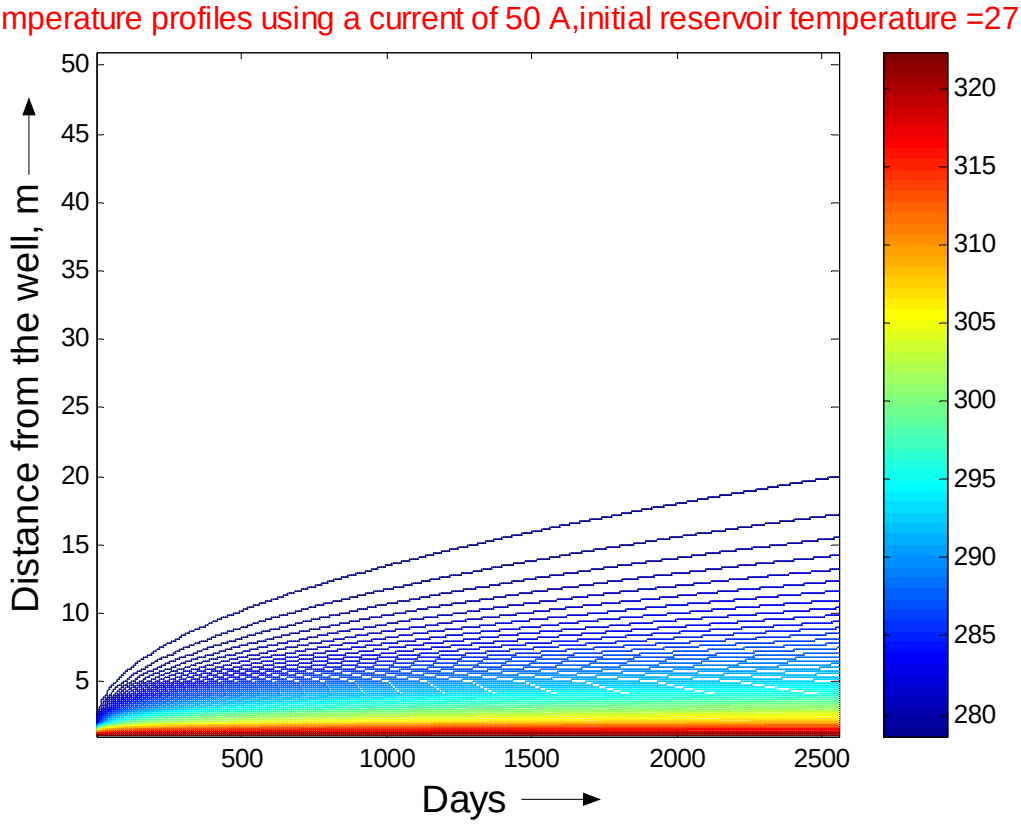

Figure 17 : Temperature profile for ohmic heating

So, the conduction equation becomes:

$$\frac{k}{\rho C_p}\frac{\partial^2 T}{\partial r^2}+\frac{k}{\rho C_p}\frac{1}{r}\frac{\partial T}{\partial r}+\frac{1}{\sigma\rho C_p}\left[\frac{I_t}{2\pi rL}\right]^2=\frac{\partial T}{\partial t} \quad (1.30)$$

The above equation is discretized by a simple FTCS (forward in time, centered in space) scheme to calculate the temperatures at various time steps for a given current level, initial reservoir temperature, electrode length and formation resistivity. Details of the parameters used are given in the Appendix.

Results of the preliminary calculation are presented in Figure 17 which shows that ohmic heating is effective in the first 10-15 meters of the well bore. The figure also shows that as with any thermal recovery methods, most of the heat input goes into heating the reservoir itself since the thermal conductivity is low. A thing which is to be noted here is the fact that the motion of the dissociation front is given by a heat (and mass) balance at the boundary between the hydrate and the dissociated free gas zone. This implies that the heat does not go directly to dissociate the hydrate; rather the dissociation profile is again influenced by the thermal conductivity of the sediment. So, it should not be construed from Figure 17 that if the temperature at a given point *r* is greater than the hydrate dissociation temperature (at the reservoir pressure), dissociation occurs; rather, the dissociation temperature (and pressure) are to be determined by an iterative procedure as given in Ref. 42.

Further work on ohmic heating was not carried out since no method to integrate depressurization with ohmic heating could be found.

6 Conclusions

It has been shown that optimal recovery and utilization of methane from hydrates is not economical with current technology. The project involved the analysis of Leg 204 data to identify the areas with higher reserves, design of a production system, development of a production model, design of processes to utilize the methane produced and an overall economic analysis.

A zero dimensional depressurization model was used to estimate the production from a vertical well at Site 1249, 1250; southern Hydrate Ridge. Based on these production rates, a simple economic analysis using Discounted Cash Flow Analysis was performed. Two cases scenarios were analyzed: (1) Production of natural gas using a FPSO with on-board Methanol production facilities, and (2) production of natural gas and further transportation using a gas-to-hydrate technology. It was found that capital and operation cost were very high, compared to total revenues from gas produced. Sensitivity analyses showed that economic feasibility (net present value) is a strong function of the selling price, either for the gas or the methanol. However, the although US natural gas demand is expected to increase from ~19.5 TCFT at present to 29.1 TCFT in 2025[37], wellhead natural gas prices are expected to increase only slightly from 3.92 $/MCF to 4.42 $/MCF in 2025[38]. This is due to projected increases in LNG imports offsetting the forecasted declines in domestic production and Canadian pipeline imports.[39]

Hence, under a scenario where wellhead natural gas prices are affected by imported LNG prices (LNG is becoming competitive compared to Canadian pipeline imports), we do not expect the price of natural gas to vary very much. Similar arguments apply to methanol, which can be obtained from a variety of sources; renewable and fossil fuel based.

We feel that the following developments in technology are needed in order to economically exploit offshore gas hydrate reserves:

1. Cheaper drilling techniques
2. Viable alternatives to floating production platforms for use with marginal, remote offshore fields.
3. Alternative methods to utilize the gas produced : subsea processing to either gas hydrate, or liquids like methanol or diesel appears attractive.
4. Better understanding of gas hydrate reservoirs from a production perspective.

That being said, we also feel that this project has been a great learning experience both in the aspect of the broad picture of hydrate science and also a lesson in team work. We thank everyone involved who contributed to this training.

[37] http://www.eia.doe.gov/oiaf/aeo/gas.html
[38] http://www.eia.doe.gov/oiaf/aeo/pdf/aeotab_14.pdf, the well head prices are in 2002 U.S. dollars.
[39] http://www.eia.doe.gov/oiaf/aeo/figure_89.html

7 Nomenclature

1. n = 1: Free gas zone
2. n = 2: Hydrate zone
3. P_e, T_e: Equilibrium pressure and temperature at the hydrate-free gas zone interface (dissociation front).
4. KN: Permeability of gas in zone *n*, 1 and 2 refer to dissociated free gas zone and undissociated hydrate zone respectively.
5. Mn: Viscosity of gas in zone *n*.
6. φ_n : Porosity of zone *n*
7. $k^{thermal}_n$: Thermal conductivity of zone *n*
8. ρ_n : Density of zone *n*
9. C_{pn}: Specific heat (at constant pressure) of zone *n*
10. α_n : Thermal diffusivity of zone *n*, $\alpha_n = k_n^{thermal} \Big/ \rho_n C_{pn}$
11. σ : Resistivity of the sediment (ohm-m)
12. I_t : Current passed (A)
13. $P_e * a_n$: Darcian Diffusivity $a_n = \dfrac{k_n}{\phi_n \mu_n}$

8 Acknowledgements

Stimulating discussions with Dr. Robert Watson helped us to get a more complete picture of the problem. We acknowledge the kind cooperation of Mr. Prasanna Chidambaram, graduate student, PNGE in providing a helpful ear to many ideas. We are also thankful to members of other teams, notably George Alexander, Marielle Narkiewicz, and Prabhat Naredi for their helpful insights, comments and knowledge sharing. Last but not the least, we are thankful to the course faculty, who motivated and kept us on track all the way to the end.

9 Appendix

A. Upstream & Hydrate Slurry

1. Permeability of clay sediments containing gas hydrates[40]:
   Taking the average grain size of clays to be 3 μm, the capillary size (diameter) is calculated to be 1.2426 μm. Using (1.31)

[40] Kleinberg R.L., Flaum C., et al., Deep Sea NMR: Methane hydrate growth habit in porous media and its relationship to hydraulic permeability, deposit accumulation and submarine slope stability; Journal of Geophysical Research (Solid Earth), 108, B10, 2508-2525

$$k_0 = \frac{\phi a^2}{8}, k_{rw} = 1-(1-S_w{}^2)+\frac{2S_w^2}{\log(1-S_w)}$$

S_w *is the water saturation*

$$k_{water} = k_o * k_{rw} \quad (1.31)$$

Where a is the capillary radius and φ is the porosity (0.65), intrinsic permeability in the absence of hydrate comes to 9.85E-14 m^2. It is known that hydrate occupies the capillary centres. The relative permeability to water is calculated by using (1.31)**Error! Reference source not found.**, with a water saturation of $S_w = 0.8$ to be 0.1647.
So, the effective permeability to water flow is 1.622e-14 m^2.

2. Simulation parameters for Ohmic Heating:
σ : 30 ohm-m[41], I_t : 50 A,
length of the horizontal well: 300 m (reservoir area is 300*500 m^2),
initial reservoir temperature : 278 K, (initial condition)
temperature at the well bore : 323 K, (boundary condition 1)
(The other boundary condition is a Von Neumann boundary condition at the end of the zone.)
thermal conductivity : 0.5 W/mK,
Density of sediment: 1500 kg/m^3, specific heat: 1600 J/kgK,
Reservoir porosity: 0.65.
Space step: 1 m, time step: 1 day, time of simulation: 7 years

3. Compression costs for natural gas are taken from the adiabatic compression from 2 MPa, 4°C to 6 MPa, accounting for 40% efficiency and are given in Table 7.
Equation used is for power calculation is:

$$Compression\ Power = \frac{P_1 * V_1}{(\gamma - 1)} * [(P_2 / P_1)^{\frac{\gamma-1}{\gamma}} - 1] \quad \gamma \text{ was taken to be } 1.33 \quad (1.32)$$

Table 7: Power requirement for compression, 1000 Nm^3/d/well

P1	2.00E+06	Pa
P2	6.00E+06	Pa
V1	4.66E+01	m3/day
gamma	1.33	
Power	1.025	kW
T1	278.000	K
T2	365.114	K
	92.114	deg C

4. The temperature of the compressed gas is assumed to rise adiabatically, this is calculated using

$$T_2 = T_1 * [(P_2 / P_1)^{\frac{\gamma-1}{\gamma}}] (1.33)$$

[41] Representative (lower end) resistivity taken from
http://www.ldeo.columbia.edu/BRG/online2/Leg204/1249A/standard/1249A-gr-rab.dat

5. Heat exchanger load/sizing calculation:

Heat Exchanger - Heat Load, Area Calculation		
U	5.000	BTU/hrft2F
Q	46.644	m3/d
	0.001	m3/s
Specific heat at constant volume	27.000	kJ/kmol-K
Molwt	32.000	kg/kgmol
Density at P2	63.247	kg/m3
Tin	92.114	C
Tout	6.000	C
mdot*Cp	0.029	kJ/K
Heat Load	2.481	kW
Water in	4.00	C
Water out	50.00	C
LMTD	13.16	C
	23.70	F
Flow rate of water	0.01	kg/s
U*LMTD	373.72	W/m2
Heat Load	2480.90	W
Area	6.64	m2
	71.45	ft2

Value of heat transfer coefficient for liquid-gas heat exchange was taken from Ref. 25. The calculation is done assuming a Z factor of 1, in reality Z~0.8.

6. Pipeline sizing calculations: (1.34)
   Assume a value of pipe diameter D

   Calculate velocity by $v = \frac{Q_{flow\ rate}}{\pi/4 * D^2}$

   Calculate Reynolds Number $\mathrm{Re} = \frac{Dv\rho_{slurry}}{\mu_{slurry}}$

   Calculate friction factor using Re:

   if Re>4000, $f = 0.079\ \mathrm{Re}^{-0.25}$, Re < 4000, $f = 16/\mathrm{Re}$

   Estimate pressure drop due to pipe friction over length L: $\Delta P = 4 f \frac{L}{D}\frac{\rho v^2}{2}$

   Estimate total head needed :H= $\frac{\Delta P}{\rho g} + Depth\ to\ seafloor(800m)$

   Estimate total power needed for pumping :Power = $\frac{\mathrm{H}\rho g Q}{\eta_{efficiency}}$

   Calculate total operating costs over 7 years using 0.03 $/kW-h : $\frac{\text{Power*24*3600*7*365*0.03}}{36e5}$ $

   Calculate total capital costs for the diameter specified : $80,000*D*100/1.6

   Calculate total costs from operating and capital costs.

   Repeat the above steps for different values of D

7. Assuming one dimensional heat and mass flows with only gas flowing through the reservoir, the following equations (along with the continuity and heat balance equations at

$$\frac{\partial P_1^*}{\partial t^*} = \frac{\partial^2 P_1^{*2}}{\partial x^{*2}} \quad \forall\ 0<\mathrm{x}<\mathrm{X_D}$$

$$\frac{\partial P_2^*}{\partial t^*} = \frac{a_2}{a_1}\frac{\partial^2 P_2^{*2}}{\partial x^{*2}} \quad \forall\ \mathrm{X_D} \le \mathrm{x}<\mathrm{L}$$

$$\frac{\partial T_1^*}{\partial t^*} - \frac{\partial P_1^*}{\partial x^*}\frac{\partial T_1^*}{\partial x^*} = \frac{\alpha_1}{P_e a_1} * \frac{\partial^2 T_1^*}{\partial x^{*2}} + \frac{1}{P_e T_e a_1 \rho_1 C_{p1}\sigma}\frac{1}{x^{*2}}\left[\frac{I_t}{Length}\right]^2 \quad \forall\ 0<\mathrm{x}<\mathrm{X_D}$$

$$\frac{\partial T_2^*}{\partial t^*} - \frac{\partial P_2^*}{\partial x^*}\frac{\partial T_2^*}{\partial x^*} = \frac{\alpha_2}{P_e a_1} * \frac{\partial^2 T_2^*}{\partial x^{*2}} + \frac{1}{P_e T_e a_1 \rho_2 C_{p2}\sigma}\frac{1}{x^{*2}}\left[\frac{I_t}{Length}\right]^2 \quad \forall\ \mathrm{X_D} \le \mathrm{x}<\mathrm{L}$$

$$a_n = \frac{k_n}{\phi_n \mu_n}$$

the dissociation front X_D) describe the temperature and pressure profiles of gas in both zones. They have been adapted from[42] . (1.35)

[42] Ahmadi G., Chuang Ji, Smith D.H., Numerical Solution for natural gas production from methane hydrate dissociation, Journal of Petroleum Science and Engineering, 41 (2004), 269-285.

B. Appendix B

Appendix B1. Energy Balance

H2	4	0	0

Heat of reaction = [2* (-110.92+(-110.5)) + 4(0)] - [2*(-51.8+(-74.83))+2*(0)]	**-72.305**	kJ/mol
No. of moles of CH4 used for syngas production	3.79E+06	kJ/day
Total heat of reaction	-2.74E+08	kJ/day
	-2.74E+05	MJ/day

Temperature increase in product stream given by

Q = mCp(T2-T1)

Q	2.74E+11	J/day				
m	10800000	mol/day			Cp*m	
Cp		CO(973) =	31.5	J/mol-K	1.13E+08	J/K
		H2(973) =	29.45	J/mol-K	2.12E+08	J/K

(T2-T1) = 841.66213

T2 1541.6621 C

Assuming 20% heat loss during heat transfer to cooling water, available heat =	2.19E+11	J/day
	2.19E+05	MJ/day

		moles	Kg
Mass entering Preheater	CH4	3.83E+06	6.12E+04
	O2	1.91E+06	6.12E+04
Total		5.74E+06	1.22E+05

Preheat Temperature = 300 C

Heat required to raise feed stream to 300 C is given below

Q = mCp(T2-T1)

Q		J/day				
m	5.74E+06	mol/day			Cp*m	
Cp		CH4(973) =	59.26	J/mol-K	2.27E+08	J/K
		O2(973) =	33.5	J/mol-K	6.41E+07	J/K

Q= 7.853E+10 J/day 908.9205995 kW power for preheating

	Total	
	2.91E+08	J/K

Appendix B1. Energy Balance Cont.1.

Water Required in FT boiler around syngas cooler

Q = (mCp1(T2-T1) + m(Hvap)+ mCp2(T3-T2))

	Q	2.19E+11	J/day			Hvap + mCp2(T2-T1)		
	Cp1	33.46	J/mol-K	1673	J/mol	45683	J/mol	
	T1	323	K					
	T2	373	K					
	Cp2	34.4	J/mol-K					
	T3	873	K					
	Hvap	44010	J/mol	1.53362E+11	J/day			
	Term 1	1673	Term 2	44010	Term 3	17200		
m		3484700.45	mol/day	62.72460809	m3/day			
		62724.60809	kg/day	2.613525337	m3/h	**3.26690667**	**m3/h**	

Available sensible heat from steam @ 600 C = 65766751584 J/day
65766.75158 MJ/day

Energy production from Methanol synthesis

CO(g) + 2H2(g) --> CH3OH(l)

Moles of Methanol produced = 3.08E+06 moles/day

Enthalpy of reaction @ ~ 150 C

Species	Moles	h in kJ/mol (298K)	h in kJ/mol (423K)
CO	1	-110.5	-110.92
H2	2	0	0
CH3OH	1	-202.091	-194.95

Heat of reaction = -128.6 kJ/mol

Total heat produced = 3.96E+08 kJ/day 3.96E+11 J/day

Assuming 20% energy loss, heat available to produce steam = 3.17E+11

Appendix Energy Balance cont2.

Temperature of steam calculated below			Heat available to produce steam - Heat required for vaporization. of water - latent heat of water Term1- Term2 - Term3				
Water							
Term 2	m	6.12E+06	mol/day	1.10E+05	kg/day water		
	Cp	33.46	J/mol-K	1.10E+02	m3/day		
	(T2-T1)	170	K	4.59E+00	m3/h	**5.74E+00**	**m3/h**
	Q	3.48E+10	J/K				
Term 3	m	4.00E+06	mol/day				
	Hvap	44010	J/mol				
	Q	1.76E+11	J/day				
Steam Temperature							
Q		1.06E+11	J/day				
m		6.12E+06	mol/day				
Cp		34.4	J/mol-K				
(T2-T1)		5.04E+02					
T2		8.77E+02	K	6.04E+02	C		
T1		373	K	100	C		

Energy converted to electricity, assuming 40% loss in steam turbines =	6.36E+10	J/day
	6.36E+04	MJ/day
Total Power that can be generated from Methanol synthesis =	1.29E+05	MJ/day
	1.50E+00	**MW**

Appendix B2: Mass Balance

Mass Balance

Syn gas production	500 C; 0.1 Mpa (1 atm)						
2CH4 + O2 --> 2CO + 4H2							
Gas production per day (ft3)		3.00E+06					
Gas production per day (m3)		8.57E+04					
No. of Moles of CH4 per day		3.83E+06					
No. of Moles of O2 required per day (assuming no excess oxygen)		1.91E+06					
Step	Loss %	**CH4**	**O2**	**CO**	**H2**	**CO + H2**	**CH3OH**
Preheater	1%	3.79E+06	1.89E+06				
Reactor	0% Conv. 5% Selectivity			3.60E+06	7.20E+06	3.60E+06	
Syn gas to Methanol	< 150 C; 5 Mpa						
Slurry Reactor	10% Conv. 5% Selectivity					3.24E+06	3.08E+06
Solvent- Product Separation	5%						2.92E+06
Methanol production rate (kg/day)							9.35E+04
CO + 2H2 --> CH3OH							
Methanol production rate (kg/day) without any loss							1.22E+05
Process Efficiency (%)							76.39211
Earnings	31120.2882 gal/day 27385.8536 $/day 9995836.57 $/year		1.14E+07 gal/year				
Assuming a total operation period of 7 years from this site	~ $ 70, 000, 000						

Appendix B3. Economic Analysis

Economic Analysis

Economic analysis of methanol production

Capital cost	MM $	
		10

This value was obtained by finding the average capital cost of methanol production units ranging from 570 t/d - 4600 t/d

ranging from 570-4600t/d

Break up of capital cost

	%	$
Steam	28	2.8
Methanol synthesis (gas to liquid)	18	1.8
Utilities	13	1.3
Offsites	14	1.4
Oxygen unit	17	1.7
Glycol separation	1	0.1
Distillation	9	0.9
	100	**10**

Rate of return (fixed cost)		1.46
Operating costs		0.75
7.5% of capital cost		
Transportation via tankers		1
Total annual costs		3.21
Marginal cost of methanol based purely on methanol production unit costs	0.276672694	$/gal

Appendix B4.Glycol Dehydration

Glycol Dehydration

Assuming a water content of 0.01M in the methane produced from gas hydrates

Production rate	85700	m3/day
	3825892.857	moles/day
Water production rate	38258.92857	moles/day
	688.6607143	kg/day

From (Makagon) 15.5 kg/day glycol to extract 28,320 SCM/day with water conc. 0.5 g/m3

Total water production	14.16	kg/day

15.5 kg glycol used to extract 14.6 kg of water

Glycol used to extract 688.66 kg water	753.8298023	kg/day
Glycol volume	0.670070935	m3/day
	176.3344567	gal/day
Glycol unit cost	$4.50	$/gal
Total glycol cost	793.505055	$/day
Assuming 90% glycol recoverability, successive cost	79.3505055	$/day
Annual glycol cost	29756.43956	
	~ $ 30,000	

Appendix B5. Catalyst& Reactor size

Catalyst & Reactor sizing

Methanol production unit

Catalyst	Slurry Phase	Reaction conditions	<150 C
Ni(CO)4	0.05 M		5 MPa
KOMe	1.0 M		
Solvent	100% THF		

Methane production per day (m3) =	85700	
Assuming 1% loss, No. of moles of gas produced per day =	3787633.93	
No. of moles of Methanol produced (calculated from mass transfer efficiency) =		3E+06
No. of moles of Methanol Produced per day =	3.07E+06	
No. of moles of Methanol Produced per hour =	1.28E+05	
Space time Yield of Catalyst (g-mol MeOH/ kg catalyst)=	570	
Catalyst amount needed for above MeOH production rate (kg) =	2.24E+02	
Density of Catalyst (assume THF density in Kg/m3) =	888	
Vol. of Catalyst required (m3)=	2.53E-01	
in Liters	2.53E+02	
Assuming 10% extra catalyst, volume required =	2.78E+02	

Since it is a slurry phase reactor, assume the entire reactor volume is occupied by catalyst and reactants.

THF required per unit MeOH produced =	6.79E-02	kg THF/ kg MeOH produced per hour)

Syngas production unit

Catalyst	Packed Bed	Reaction conditions	500 C
	Ni		0.1 MPa (1 atm)
Support	Alumina		

Reactants flow rate (moles) per day =

CH4	3.76E+06
O2	1.88E+06

Reactant flow rates (moles) per hour =

CH4	1.57E+05
O2	7.83E+04

Total reactant moles per hour = 2.35E+05

Appendix B5. Catalyst & reactor size

GHSV (h-1) of Catalyst based on reaction kinetics ~ 500 C =	1.40E+05
Catalyst volume (L)=	3.76E+01
in m3 =	3.76E-02
Density of catalyst (assume close to Ni Density) in kg/m3 =	3.90E+03
Mass of Catalyst required in kg =	1.61E+02

Reactor Sizing

Assuming 10% extra Volume of catalyst, we require (in L) =	4.14E+01
Assuming 10% extra Volume in the inlet & outlet, we require (in L) =	4.96E+01

cost ref : http://www.eere.energy.gov/hydrogenandfuelcells/pdfs/merit03/3_nrel_kim_magrini_bair.pdf

Appendix B6. Production Model MatLab® Code

```
********************************************************************************
**********DESCRIPTION OF THE PROGRAM*****************************
```

Zero-dimensional depressurization model for the production of natural gas from a natural gas hydrate reservoir. Based on paper published by Santanu Khataniar, The Canadian Journal of Chemical Engineering, Volume 80, February 2002. Assumptions: (1) Reservoir behaves as a tank model with a centrally located production well; (2) Instantaneous equilibrium is achieved through the gas zone; (3) Hydrate decomposition follows Kim's model; (4) Connate water and rock expansion are negligible; (5) No external water drive exist; (6) Neglection of heat transfer from surroundings.

```
********************************************************************************
**********************************AUTHOR****************************************
```

Team 2: Gong Y., Indrakanti V.P., Perez P., Powers S., Venkataraman R.
FSc 503, Fall 2004
Programmed by: Peter Perez

```
********************************************************************************
```

CONSTANTS AND CONVERSION FACTORS

```
A=150,000;          %Hydrate Reservoir Area, m2
Ghi=14e9;           %Initial Hydrated Gas in Place, m3
Gfi=4e9;            %Initial Free Gas in Place, m3
Pi=10000;           %Initial Reservoir Pressure, KPa
hh=110.0;           %Hydrate Zone Average Thickness, m
hg=10.0;            %Free Gas Zone Thickness, m
phif=0.04;          %Reservoir Porosity (Free gas zone), %
phih=0.20;          %Reservoir Porosity (Hydrate zone), %
Swf=0.85;           %Initial Water Saturation (Free gas zone), %
Swh=0.10;           %Initial Water Saturation (Hydrate zone), %
T=10;               %Initial Average Reservoir Temperature, C
Pw=2000;            %Flowing Well Bottomhole Pressure, KPa
c=0.00026;          %Well Deliverability Constant, m3/s-KPa
n=0.5;              %Well Deriverability Exponent, dimensionless
Bgh=0.0061;         %Hydrate Formation Volume Factor, SCM/m3
Bw=1.00;            %Water Formation Volume Factor, SCM/m3
ER=16950;           %Activation Energy of Hydrates, R
ko=2681;            %Hydrate Decomposition Equilibrium Constant, SCM/m2.s.Pa
kw=0.01*1e-15;      %Effective Permeability of Water, m2
kg=10.0*1e-15;      %Effective Permeability of Gas, m2
mug=1.0e-5;         %Viscosity of Gas, Pa.s
muw=1.3e-3;         %Viscosity of Water, Pa.s
Tsc=273;            %Standard Temperature, K
Psc=101325;         %Standard Pressure, Pa
Zsc=1.00;           %Gas Compressibility at Standard Conditions, dimensionless
Ppc=668;            %Methane Critical Pressure, psi
Tpc=343;            %Methane Critical Temperature, R
```

INITIATION VALUES FOR ITERATION

```
t=0;
P=Pi;
counter=0;

for P_new = Pi: -100: Pw;
   counter = counter + 1;
```

FIND REDUCED DENSITY: NEWTON-RAPHSON METHOD

```
t_factor=Tpc/((1.8*T+32)+460);                    %R=F+460
Ppr=(P*0.1450)/Ppc;                               %1 KPa = 0.1450 psi
y=0.02;

Ft=-0.06125*Ppr*t_factor*exp(-1.2*(1-t_factor)^2)+(y+y^2+y^3-y^4)/(1-y)^3-(14.76*t_factor-
9.76*t_factor^2+4.58*t_factor^3)*y^2+(90.7*t_factor-
242.2*t_factor^2+42.4*t_factor^3)*y^(2.18+2.82*t_factor)

while abs(Ft)>0.000000000001;

y_new=y-Ft/((1+4*y+4*y^2-4*y^3+y^4)/(1-y)^4-(29.52*t_factor-
19.52*t_factor^2+9.16*t_factor^3)*y+(2.18+2.82*t_factor)*(90.7*t_factor-
242.2*t_factor^2+42.4*t_factor^3)*y^(1.18+2.82*t_factor));

y=y_new;
end
```

COMPUTE GAS COMPRESSIBILITY (Z-FACTOR)

```
Z=0.06125*Ppr*t_factor*exp(-1.2*(1-t_factor)^2)/y;          %Gas Compressibility at T and P
```

COMPUTING PRESSSURE PROFILES FROM STANDARD BACKPRESSURE EQUATION:

```
Bg=(((P*1000)*Tsc*Zsc)/(Psc*(T+273)*Z))^(-1);              %Gas Expansion Volume Factor.

dBgdP=-( Psc*T/(Tsc*Zsc)*(-Z/(1000*P)^2+(1/(1000*P))*(0.06125*t_factor*exp(-1.2*(1-
t_factor)^2)/(y*Ppc))) );                                  %Derivative of Bg respect to P

Peq=10^(0.0342*((T+273.15)-273.15)+0.0005*((T+273.15)-273.15)^2+6.4804);    %Dissociation Pressure

 Qg=( c*(P^2-Pw^2)^n );                                    %Gas Production Rate, m3/s

   if 1000*P >= Peq;
     J=0;
   else
     J=1;
   end

dGehdt=ko*A*phih*exp(-ER/((1.8*T+32)+460))*(Peq-P*1000)*J;       %Gas Influx from Hydrates, m3/s

dPdt=( (Qg*Bg*(1+kw*mug/(kg*muw))-(Bg-Bgh+8.33e-4*Bw)*dGehdt*J)/(A*phif*(1-
Swf)*hg*(1/Bg)*dBgdP) );                                    %Depressurization Rate in Pa/s

dhdt=-( ko*exp(-ER/((1.8*T+32)+460))*(Peq-P*1000)*Bgh*J/(1-Swh) );
```

COMPUTING TIME PROFILES:

```
t_new=t + ( (P_new-P)*1000/dPdt );
t=t_new;
P=P_new;
h=hh+dhdt*t;                    %Variation of Hidrate Zone Thickness, m
Gph=dGehdt*t*J;                 %Cumulative Production from Hydrates, m3
Gp=Qg*t+dGehdt*t*J;             %Total Cumulative Production, m3
dGpf=Qg-dGehdt;                 % Production Rate from Free Gas, m3/s
Gpf=Gp+Gph;                     %Cumulative Production from free gas, m3
f=Gph/Gp;                       %Percent Contribution from Hydrates, %
Qw=8.33e-4*dGehdt;              %Water Production Rate, m3/s
Wp=Qw*t;                        %Cumulative Water Production, m3
```

COMPUTING VECTORS:

```
hvec(counter)=h;                                %m
dhvec(counter)=dhdt;                            %m/s
tvec(counter)=t/(24*3600*365);                  %years
pvec(counter)=P_new;                            %KPa
qvec(counter)=Qg*3600*24*35.31;                 %SCFD
dGhvec(counter)=dGehdt*3600*24*35.31;           %SCFD
dPvec(counter)=dPdt;                            %Pa/s
Gpvec(counter)=Gp*35.31;                        %SCFD
Gpfvec(counter)=Gpf*35.31;                      %SCF
dGpfvec(counter)=dGpf*3600*24*35.31;            %SCFD
Gphvec(counter)=Gph*35.31;                      %SCFD
fvec(counter)=f*100;                            %Percent (%)
qwvec(counter)=Qw*3600*24*35.31;                %CFD
wpvec(counter)=Wp*35.31;                        %CF

end
```